T.C.
DOKUZ EYLÜL UNIVERSITY IZMIR INTERNATIONAL BIOMEDICINE AND GENOME INSTITUTE

INTERACTIONS OF ELF3 AND DNA METHYL TRANSFERASES IN MESENCHYMAL EPITHELIAL TRANSFORMATION

SERAY YETKİN

DEPARTMENT OF GENOMICS AND MOLECULAR BIOTECHNOLOGY

Molecular Biology and Genetics

MASTER OF SCIENCE THESIS

IZMIR-2023

THESIS CODE: DEU.IBG.MSc-2021850006

T.C.

DOKUZ EYLÜL UNIVERSITY IZMIR INTERNATIONAL BIOMEDICINE AND GENOME INSTITUTE

INTERACTIONS OF ELF3 AND DNA METHYL TRANSFERASES IN MESENCHYMAL EPITHELIAL TRANSFORMATION

SERAY YETKİN

DEPARTMENT OF GENOMICS AND MOLECULAR BIOTECHNOLOGY

Molecular Biology and Genetics

MASTER OF SCIENCE THESIS

Supervisor: Assoc. Prof. Hani Alotaibi

This work was supported by

TÜBİTAK grant 120N556

IZMIR-2023

THESIS CODE: DEU.IBG.MSc-2021850006

Dokuz Eylül University Izmir International Biomedicine and Genome Institute

Department of Genomics and Molecular Biotechnology, Molecular Biology and Genetics graduate program Master of Science student SERAY YETKİN has successfully completed her Master of Science thesis titled "**INTERACTIONS OF ELF3 AND DNA METHYL TRANSFERASES IN MESENCHYMAL EPITHELIAL TRANSFORMATION**" on the date of 08/09/2023.

Assoc. Prof. Hani Alotaibi
Dokuz Eylül University CHAIR

Assoc. Prof. Gökhan Karakülah
Dokuz Eylül University
MEMBER

Asst. Prof. Ayşe Banu Demir
Izmir University of Economics
MEMBER

Asst. Prof. Yavuz Oktay
Dokuz Eylül University
SUBSTITUTE MEMBER

Prof. Ralph Muewissen
Ege University
SUBSTITUTE MEMBER

Dokuz Eylül Üniversitesi İzmir Uluslararası Biyotıp ve Genom Enstitüsü Genom Bilimleri ve Moleküler Biyoteknoloji Anabilim Dalı, Moleküler Biyoloji ve Genetik Yüksek Lisans programı öğrencisi, SERAY YETKİN "**INTERACTIONS OF ELF3 AND DNA METHYL TRANSFERASES IN MESENCHYMAL EPITHELIAL TRANSFORMATION**" konulu Yüksek Lisans tezini 08/09/2023 tarihinde başarılı olarak tamamlamıştır.

Doç. Dr. Hani Alotaibi

Dokuz Eylül Üniversitesi

BAŞKAN

Doç. Dr. Gökhan Karakülah	Dr. Öğr. Üyesi Ayşe Banu Demir
Dokuz Eylül Üniversitesi	Izmir Ekonomi Üniversitesi
ÜYE	ÜYE
Dr. Öğr. Üyesi Yavuz Oktay	Prof. Ralph Muewissen
Dokuz Eylül Üniversitesi	Ege Üniversitesi
YEDEK ÜYE	YEDEK ÜYE

TABLE OF CONTENTS

TABLE OF CONTENTS I
LIST OF TABLES IV
LIST OF FIGURES V
LIST OF ABBREVIATIONS VI
ACKNOWLEDGMENTS ....
VII ABSTRACT
....
1 ÖZET
.... 2
1. INTRODUCTION 3
1.1. Statement and Importance of the Problem 3
1.2. Aim of Study 3
1.3. Hypothesis of Study 4
2. GENERAL INFORMATION 5
2.1. Cellular Plasticity 5
2.2. Epithelial-Mesenchymal Transition and Mesenchymal-Epithelial Transition 6
2.2.1 Epithelial-Mesenchymal Transition (EMT) 6
2.2.2 Mesenchymal Epithelial Transition (MET) 7
2.3. Transcriptional Regulation of EMT 8

2.4. Transcriptional Regulation of MET 9

2.4.1 Grhl3 10

2.4.2 Hnf4α 10

2.4.3 Elf3 11

2.5. Epigenetic Regulation of EMT/MET 12

2. MATERIALS AND METHODS 14

3.1. Type of Study 14

3.2. Time and Place of Study 14

3.3. Materials of Study 14

3.3.1 Cell Culture Materials, Reagents & Cell Lines 15

3.3.2 PCR, cDNA, and qPCR Reagents 15

3.3.3 siRNA Sequence Information 15

3.3.4 Immunofluorescence Labelling Reagents 16

3.3.5 Plasmid Construction 16

3.3.6 Molecular Cloning Reagents 17

3.3.7 Bacterial Reagents 17

3.3.8 ChIP Reagents 17

3.3.9 Methylated DNA Immunoprecipitation- hydroxymethylated DNA Immunoprecipitation (MeDIP-hMeDIP) Reagents 18

3.3.10 Other Chemicals, Consumables, and Commercial Kits 18

3.3.11 Hardware & Machines 18

3.3.12 Chemical Recipes 19

3.4. Variables of Study 21

3.5. Tools For Data Collection 21

3.6 Study Plan and Calendar 21

3.7 Data Evaluation 21

3.7.1 Cell Culture and EMT/MET Experiment Model 21

3.7.2 siRNA Knockdown and mRNA Expression Analysis 22

3.7.3 RNA-seq Data Analysis 22

3.7.3.1 Raw Data Processing 22

3.7.3.2 Differential Expression Analysis 22

3.7.3.3 Visualizations 23

3.7.4 Immunofluorescence Labeling and Confocal Microscopy 23

3.7.5. Conservation Analysis 23

3.7.6 Construction of Reporter Vector Sequences 23

3.7.7 Luciferase Reporter Activity Measurement 24

3.7.8 Chromatin Immunoprecipitation (ChIP) 24

3.7.9 Methylated DNA Immunoprecipitation and hydroxymethylated DNA Immunoprecipitation (MeDIP-hMeDIP) 24

3.8. Limitation of the Study 25

3.9. Ethics Committee Approval 25

4. RESULTS 26

4.1. Elf3 Silencing Alters MET 26

4.1.1. mRNA Expression Analysis in Response to Elf3 Silencing 26

4.1.2. Immunofluorescence Labeling and Confocal Microscopy 28

4.2. RNA-seq Data Analysis 29

4.2.1. Preprocessing and Alignment of Sequencing Reads 29

4.2.2. Differential Expression Analysis in Response to Elf3 Silencing During MET 30

4.2.3. Gene Ontology Analysis 31

4.2.4. Gene Set Enrichment Analysis 32

4.3. Elf3 as a Regulator of DNA Methyltransferases 34

4.3.1. Conservation Analysis and Construction of Reporter Vectors 34

4.3.2. Luciferase Reporter Activity Measurement 37

4.3.3. Chromatin Immunoprecipitation (ChIP) 39

4.4. Methylated DNA Immunoprecipitation-hydroxymethylated DNA Immunoprecipitation (MeDIP-hMeDIP) 40

5. DISCUSSION 44

6. CONCLUSION AND SUGGESTIONS 48

7. REFERENCES 49

8. APPENDIX 60

LIST OF TABLES

Table 1. Cell culture reagents 15
Table 2. PCR, cDNA, and qPCR Reagents 15
Table 3. siRNA Sequence 15
Table 4. Immunofluorescence Labelling Reagents 16
Table 5. Molecular Cloning Reagents 17
Table 6. Bacterial Reagents 17
Table 7. ChIP Reagents 17
Table 8. meDIP and hmeDIP Reagents 18
Table 9. Other Chemicals, Consumables, and Commercial kits 18
Table 10. Hardware and machines used in this study 19
Table 11. Alignment statistics of siCntrl and siElf3 samples for each replicate. 29
Table 12. Number of differentially expressed protein-coding and long non-coding RNAs in response to Elf3 silencing. 31
Table 13. Cloning Primer Sequences with restriction sites. 60
Table 14. qPCR Primers and Probe informations. 60

LIST OF FIGURES

Figure 1. Illustration of EMT and MET by showing the effect of Elf3 knockdown. 12
Figure 2. The EMT-MET processes were visualized using immunofluorescent staining. 14
Figure 3. pGL4.10 plasmid construction. 16
Figure 4. The expression levels of Epithelial genes during EMT-MET. 26
Figure 5. The expression levels of Mesenchymal genes during EMT-MET. . 27
Figure 6. The siRNA-mediated silencing of Elf3. 27
Figure 7. The siRNA-mediated silencing of Elf3 the immunofluorescence

staining of NMuMG cells in EMT-MET. 28
Figure 8. Principal Component Analysis ....
30
Figure 9. Volcano plot. ....
31
Figure 10. Barplot shows top 25 significant GO terms enriched for Biological Process in response to Elf3 silencing. 32
Figure 11. Gene Set Enrichment Analysis. 33
Figure 12. Heatmap representing the expression variances of interested genes ....
34
Figure 13. The Elf3 binding site profile as presented by the JASPAR database.
.... 35
Figure 14. Conserved Elf3 binding sites in the Dnmt1 promoter. 36
Figure 15. Conserved Elf3 binding sites in the Uhrf1 promoter. 36
Figure 16. Conserved Elf3 binding sites in the Dnmt3b promoter. 37
Figure 17. Luciferase reporter assay showing the activation of promoters by Elf3. ....
38
Figure 18. Agarose gel electrophoresis gel image for ChIP. 39
Figure 19. Elf3 binding at the promoters of Dnmt1, Dnmt3b, and Uhrf1. 39
Figure 20. Agarose gel electrophoresis gel image for DIP. 40
Figure 21. Methylation states of epithelial genes during EMT-MET. 41
Figure 22. The methylation states of mesenchymal genes during EMT-MET
....
42
Figure 23. Promoter methylation of epithelial genes in response to Elf3 silencing during MET. 43
Figure 24. Promoter methylation of mesenchymal genes genes in response to Elf3 silencing during MET. 43

LIST OF ABBREVIATIONS

NMuMG: **N**ormal **Mu**rine **M**ammary **G**land

EMT: Epithelial-Mesenchymal Transition

MET: Mesenchymal-Epithelial Transition E-cadherin:

Epithelial cadherin

N-cadherin: Neural cadherin

RPKM: Reads mapped Per Kilobase of transcript per Million Mapped reads

TGFβ: Transforming Growth Factor Beta

GSEA: Gene set enrichment analysis

GO: Gene ontology

DIP-seq: DNA Immunoprecipitation sequencing dNTP:

Nucleoside Triphosphate ddNTP:

Dideoxyribonucleotide Triphosphate

GRNs: Gene regulatory networks lncRNA:

Long Noncoding RNA

ACKNOWLEDGMENTS

I am fortunate to have received support from my supervisor, friends, and family. I'd like to express my gratitude to each of them for their assistance and understanding with this thesis research:

First and foremost, my supervisor, Assoc. Prof. Hani Alotaibi, for his encouragement and guidance. He showed me how to be patient, gave me advice, and made valuable observations, suggestions, and recommendations. I firmly maintain that the extensive knowledge I learned and will learn from him will shed light on my career path in this science journey.

Assoc. Prof. Gökhan Karakülah, for his support and continued guidance.

I'd like to extend my thanks to all members of the Alotaibi lab, past and present, with whom I have crossed paths. Specifically, I want to acknowledge Ayça, Büşra, and Şeyma for their immediate support during stressful times. I'd also like to express my gratitude to Tuğçe, Gkamze, and Mehdi for their friendly faces, friendship, and support. In academia, friends are indispensable, and I'm unsure how far I could have gone without them.

Lastly, but by no means less important, I would like to express my gratitude to my parents, Bülent and Fahriye Yetkin, my beloved brother and hommie Deniz Yetkin, for their unfailing love and unconditional support throughout my life. They nurtured my success with boundless love, trust, and endless patience. I also want to thank my uncle, E. Fatih Yetkin, for his valuable and infinite academic advice. Thank you for being an excellent role model for me. I am very grateful for my family's encouragement, which entertained and helped me overcome this difficult time most positively and efficiently.

INTERACTIONS OF ELF3 AND DNA METHYL TRANSFERASES IN MESENCHYMAL EPITHELIAL TRANSFORMATION

Seray Yetkin, İzmir International Biomedicine and Genome Institute, Dokuz Eylul University Health Campus, Balcova 35340 - Izmir / TURKEY

ABSTRACT

Mesenchymal-epithelial transition (MET) and Epithelial-mesenchymal transition (EMT) processes are two biological events important for many critical physiological and pathological processes such as embryonic development, wound healing, and tumorigenesis. MET has until recently been viewed only as the reverse process of EMT. However, recent studies indicate that MET is not simply the reverse of EMT. Elf3 plays a role in regulating MET by changing the expected localization of E-cadherin on the plasma membrane and regulating Grhl3 expression by binding to conserved sequences within the Grhl3 promoter. The loss of Elf3 expression in the cell impairs MET initiation and causes cells to remain mesenchymal; a positive feedback network involving Elf3 seems very likely. DNA methylation is one of the most important epigenetic modifications determining cellular identity in the MET process, catalyzed by DNA methyl transferases (DNMT). DNA methylation and hydroxymethylation have been the focus of attention due to their biological and epigenetic roles in cellular systems, including differentiation, development, and pluripotency, and have been shown as an intermediate step in the active DNA demethylation reaction. In this context, this thesis aimed to investigate the possible interplay between DNA methylation enzymes and Elf3, which plays an essential role during MET. We applied an integrated approach, including gene modulation, DNA-protein interaction, and bioinformatics. The results indicated that Elf3 is involved in the transcriptional regulation of DNA methyltransferases, extending the roles of Elf3 in the regulation of MET and illuminating novel functions of Elf3. The findings also increased our epigenetic perspective on the regulation of MET.

Keywords: MET, Transcriptional Networks, EMT, Elf3, DNA Methylation, Epigenetics

MEZENKİMAL EPİTELYAL DÖNÜŞÜM SÜRECİNDE ELF3 VE DNA METİL TRANSFERAZLARIN ETKİLEŞİMLERİ

Seray Yetkin, İzmir Uluslararası Biyotıp ve Genom Enstitüsü, Dokuz Eylül Üniversitesi Sağlık Yerleşkesi, Balçova 35340 - İzmir / TÜRKİYE

ÖZET

Mezenkimal-epitelyal geçiş (MET) ve Epitelyal-mezenkimal geçiş (EMT) süreçleri, embriyonik gelişim, yara iyileşmesi ve tümör oluşumu gibi birçok kritik fizyolojik ve patolojik süreç için önemli olan iki biyolojik olaydır. MET yakın zamana kadar yalnızca EMT'nin ters süreci olarak görülüyordu. Ancak son araştırmalar MET'in sadece EMT'nin tersi olmadığını göstermektedir. Elf3, Ekadherin'in plazma zarı üzerindeki beklenen lokalizasyonunu değiştir ve Grhl3 promotörü içindeki korunmuş dizilere bağlanır. Böylelikle Grhl3 ekspresyonunu değiştirerek MET'in düzenlenmesinde rol oynar. Hücrede Elf3 ekspresyonunun kaybı MET başlatılmasını bozarak hücrelerin mezenkimal kalmasına neden olur; Elf3'ü içeren pozitif bir geri bildirim ağı çok muhtemel görünmektedir. DNA metilasyonu, DNA metil transferazlar (DNMT) tarafından katalize edilen MET sürecinde hücresel kimliği belirleyen en önemli epigenetik modifikasyonlardan biridir. DNA metilasyonu ve hidroksimetilasyonu, hücresel sistemlerde farklılaşma, gelişme ve pluripotens dahil olmak üzere biyolojik ve epigenetik rolleri nedeniyle ilgi odağı olmuş ve aktif DNA demetilasyon reaksiyonunda bir ara adım olarak gösterilmiştir. Bu bağlamda bu tez, DNA metilasyon enzimleri ile MET sırasında önemli bir rol oynayan Elf3 arasındaki olası etkileşimin araştırılmasını amaçlamıştır. Gen modülasyonu, DNA-protein etkileşimi ve biyoinformatiği içeren entegre bir yaklaşım uyguladık. Sonuçlar, Elf3'ün, DNA metiltransferazların transkripsiyonel düzenlemesinde yer aldığını, Elf3'ün MET düzenlemesindeki rollerini genişlettiğini ve Elf3'ün yeni fonksiyonlarını aydınlattığını gösterdi. Bulgular aynı zamanda MET'in düzenlenmesine ilişkin epigenetik bakış açımızı da arttırdı.

Anahtar kelimeler: MET, Transkripsiyonel Ağlar, EMT, Elf3, DNA Metilasyonu, Epigenetik

1. INTRODUCTION

1.1. Statement and Importance of the Problem

Epithelial-mesenchymal transition (EMT) and mesenchymal-epithelial transition (MET) are two cellular reprogramming events and they are interrelated but not directly antagonistic processes. These processes are pivotal in various multicellular organism events, including gastrulation, organogenesis, and wound healing. The early research on MET assumed that these two processes shared a common regulatory network, and MET was perceived as a natural consequence of either suppressing EMT or removing factors that induce EMT. However, contemporary understanding reveals that MET is governed by a distinct core regulatory network different than EMT. This underscores the complexity of MET, which is more intricate than initially believed. Protein-coding genes and the transcription factors that control their expression have been the subject of the few research that have been conducted on MET regulation. There has been a notable absence of research investigating the DNA methylation during MET and the extended functions of the Elf3 transcription factor. It is crucial to acknowledge the substantial impact of transcription factors on epigenetics to understand gene regulation comprehensively in the context of EMT and MET processes.

1.2. Aim of Study

This Project mainly aims to investigate the impact of Elf3 on DNA methylation and DNA methyltransferases (Dnmt1, Dnmt3b, Uhrf1) using an integrated approach, including gene modulation and bioinformatics, and to contribute to our epigenetic perspective in the regulation of MET with in vitro experiments to be performed on the NMuMG cell line.

Aim:

To study the state of DNA methylation and hydroxymethylation of epithelial and mesenchymal genes influencing EMT and MET and to define the role of Elf3 in DNA methylation.

Objectives:

1. To define the transcriptional relationships between Elf3 and DNA methyltranferases using the RNAi-mediated gene silencing in MET.

2. To determine the transcriptional regulation of DNA methyltransferases by Elf3.

3. To study the impact of Elf3 silencing on DNA methylation and hydroxymethylation during the MET.

1.3. Hypothesis of Study

The proper regulation of Cdh1 expression is crucial for the successful progression of both EMT and MET. During EMT, the downregulation of Ecadherin can be attributed to its suppression by the EMT-inducing factors and the release of activators that act on its promoter region. The reactivation of Ecadherin during MET can be explained by the presence of transcriptional activators, which may also function as regulators of MET. Previously our laboratory investigations have demonstrated that the loss of Elf3 expression in cells hinders the initiation of MET, causing cells to remain in a mesenchymallike state. This suggests the existence of a positive feedback network involving Elf3, which plays a crucial role in MET. Furthermore, the transcription of DNA methyltransferases appears to be influenced by the absence of Elf3. With this knowledge in mind, the DNA methylation and hydroxymethylation patterns associated with MET, could be in part regulated by Elf3, and in the absence of Elf3 this could lead to significant alterations in the epigenetic landscape.

2. GENERAL INFORMATION

2.1. Cellular Plasticity

Cellular plasticity plays a pivotal role in embryogenic development through intricate cell interactions (Iacono et al., 2017; Keller, 2005; Newman, 2020). Gene regulatory networks (GRNs) regulate dynamic modifications governing various changes. Consequently, the regulation of gene expression is critical for differentiation and development. GRNs control phenotypic shifts in response to environmental variability via epigenetic modifications, leading to phenotypic diversification (Jia et al., 2017; Thomas et al., 2014). This interplay between molecular entities: genes, proteins, microRNAs, and lncRNAs within GRNs drives plasticity between stable and intermediate cell states (Gupta et al., 2019; Teeuwssen and Fodde, 2019).

Epigenetic mechanisms, such as the dynamic modulation of DNA methylation and histone modifications, significantly regulate gene expression (Gibney and Nolan, 2010). The cooperative interplay of these epigenetic mechanisms with genetic factors heightens the complexity of cellular plasticity's regulatory landscape. Cellular plasticity programs enable epigenomic modulation, which alters gene expression while preserving genotypes (Duncan et al., 2014; Tian and Marsit, 2018), orchestrated through conserved and complex mechanisms (Gibson, 2008; Lavin and Tiwari, 2020; Varga and Greten, 2017).

Cell adhesion significantly shapes cellular morphology and interactions, regulated by E-cadherin (E-cad) (Erami et al., 2015; van Roy and Berx, 2008). Controlled modulation of Cdh1 is indispensable for the plasticity and dynamic changes crucial in numerous biological processes (Kroepil et al., 2012). Although the reduction of E-cadherin is a hallmark of epithelial-mesenchymal transition (EMT), both EMT and Mesenchymal Epithelial Transition (MET) are intricately linked to cancer-related cellular plasticity (Bakir et al., 2020; Chaffer et al., 2016). In carcinogenesis and immune surveillance, interactions between cancer cells exhibiting EMT and MET-related plasticity and the immune microenvironment hold paramount importance. Evidence suggests EMT promotes cancer cell dissemination and metastatic colonization, involving entities like breast cancer cells, tumor-associated macrophages, and hepatic progenitor cells (Giannelli et al., 2016; Lin et al., 2019).

Cellular plasticity-mediated transitions between epithelial and mesenchymal states contribute to heterogeneity across various cancer types (T. Chen et al., 2017). Besides cancer-initiating cells, the tumor microenvironment features non-cancerous cells like fibroblasts and immune cells (De Jaeghere et al., 2019; Gajewski et al., 2013). Cross-communication between cancer cells and the immune microenvironment, with inherent cellular plasticity during EMT-MET, significantly impacts tumor initiation and immune surveillance. EMT-inducing pathways like TGF-β and Wnt drive epithelialmesenchymal plasticity by modulating inducers, including Zeb1/2 and Snai1, conferring cancer dissemination and immune evasion properties (Jia et al., 2019; Jing et al., 2011).

2.2. Epithelial-Mesenchymal Transition and Mesenchymal-Epithelial Transition

Epithelial cells are characterized by their well-defined apical-basal polarity, while in contrast, mesenchymal cells adopt a clustered arrangement with limited adhesion among individual cells, leading to a non-polarized state (S. S. Choi and Diehl, 2009). Epithelial cells tightly engage with their neighboring cells, forming robust connections and adhering to the cellular membrane. This distinct apicobasal polarity is a hallmark of epithelial cells. In contrast, mesenchymal cells lack such robust physical interactions with neighboring cells, rendering them more susceptible to migration and movement (Shu and Pei, 2014). EMT and MET are fundamental processes characterized by dynamic alterations in cellular identity without genomic changes (Lamouille et al., 2014). Epithelial cells exhibit strong apical-basal polarity, while mesenchymal cells lack such polarization, allowing them to act individually due to reduced intercellular connectivity (Nelson, 2009). During EMT, polarized epithelial cells undergo substantial transcriptional and posttranscriptional changes to adopt a mesenchymal phenotype. Key features of EMT and MET encompass altered gene expression of cell adhesion molecules, cytoskeletal reorganization, and modulation. Although EMT and MET are interdependent processes, they differ notably, particularly in the roles of the regulatory partners involved.

2.2.1 Epithelial-Mesenchymal Transition (EMT)

Throughout embryonic development, cell states dynamically shift by harnessing cellular plasticity. Epithelial cells demonstrate remarkable plasticity during embryonic morphogenesis processes, such as forming the mesoderm and neural crest transitioning into mesenchymal cells through the process known as EMT (Thiery et al., 2009). It represents a reversible molecular program that prompts cells to embrace an invasive, non-polarized mesenchymal identity by relinquishing their characteristic polarized morphologies (Diepenbruck and Christofori, 2016). EMT is essential across various biological processes, including embryogenesis and cancer development (Thiery et al., 2009).

Throughout EMT, cell interactions undergo a profound reshaping, and the transcriptional machinery undergoes alterations to steer cellular fate (J. Chen et al., 2012). EMT elicits substantial changes in about 10% of the human genome, coupled with cytoskeleton rearrangements.

These extensive shifts in gene expression during EMT are underpinned by a complex interplay of signaling molecules, mediators, and regulators, which can be categorized into EMT effectors, EMT core regulators, and EMT inducers (Lamouille et al., 2014). The transition involves the loss of cellular polarity, the characteristic adherent morphology, and the expression of epithelial genes, orchestrated through the downregulation of cell adhesion molecules like E-cad, fibronectin, and N-cadherin, crucial for driving cell migration and invasion (Lamouille et al., 2014). Notably, E-cad experiences a critical downregulation during EMT (Lombaerts et al., 2006), with its expression restored promptly during the subsequent MET.

The induction of EMT is organized by diverse signaling cues, often activating intracellular EMT inducers such as Snai1/2, Twist, and Zeb1/2, comprising a core transcriptional regulatory network that governs the EMT program (Fazilaty et al., 2019; Lavin and Tiwari, 2020). These EMT core regulators, functioning as transcription factors, contribute to the repression of E-cad expression. They bind to evolutionarily conserved E-boxes located in the proximal promoter of Cdh1 (Canel et al., 2013). In contrast, the second intron of E-cad has emerged as a pivotal regulator of Cdh1 expression (Stemmler et al., 2005).

While the induction of EMT is context-dependent and varies among cell types, crucial signaling pathways such as TGFβ, Wnt, and Notch play roles in EMT induction (Lamouille et al., 2014; J. Zhang et al., 2016). TGFβ signaling is a central player in EMT, directly activating core EMT regulators (Snail, Slug, Twist, Zeb1/2) (Wendt et al., 2009; Xu et al., 2009). TGFβ is pivotal in critical cellular functions such as proliferation, differentiation, and apoptosis in adult and embryonic cells (Lafontaine et al., 2011; Ramesh et al., 2009; Y. Zhang et al., 2017). The interplay between TGFβ and Smad signaling in driving EMT is intricately connected to other pathways, such as PI3K and MAPK (Chapnick et al., 2011; H. Zhang et al., 2009). TGFβ fosters enhanced cell motility, invasion, and metastasis during EMT (Massague, 2008).

EMT is classified into three types based on its context and origin: Type I EMT is pivotal in developmental processes like mesoderm formation, neural crest delamination, heart valve establishment, palatogenesis, and myogenesis. Type II EMT activates during fibrosis and wound healing in response to tissue damage. Type III EMT, pertinent to tumorigenesis, triggers cancer cell dissemination, invasion, and metastasis (Sisto et al., 2018; Thiery et al., 2009).

2.2.2. Mesenchymal Epithelial Transition (MET)

Maintaining equilibrium between the EMT and MET programs is crucial for most cellular processes (Roca et al., 2013). Previously, MET was primarily seen as the reverse of EMT. While reduced E-cad expression and suppression of EMT inducers like Zeb1/2 and Snai1/2 hallmark EMT (Adhikari et al., 2014), MET extends beyond EMT inducers. Numerous transcription factors (TFs) function as molecular switches, intricately guided by epigenetic mechanisms, to sustain cellular plasticity (J. Choi et al., 2017; Skrypek et al., 2017). This underscores that MET is not solely the inverse of EMT but rather a central program. A number of dynamic, carefully controlled events involving transcriptional and post-transcriptional pathways are required for the beginning and maintenance of Cdh1 gene expression and the presence of E-cad on the plasma membrane (Sengez et al., 2019). The significance of MET has come to light recently. While it has been newly recognized as a pivotal reprogramming event, the precise mechanisms governing MET remain unclear.

E-cadherin, which is suppressed during EMT, experiences swift restoration during MET. This shift involves heightened epithelial gene expression alongside diminished mesenchymal gene expression, allowing cells to regain their apicobasal polarity (Yao et al., 2011). Reactivation of Ecad expression stands as a critical step of MET. Several studies suggest that a decrease in the expression of core EMT regulators and their detachment from the Cdh1 promoter region alone does not sufficiently account for the rapid activation of the Cdh1 locus during MET (Alotaibi et al., 2015; Stemmler et al., 2005, 2003). The release and downregulation of these repressors during MET may serve to explain some of the initial activation of the Cdh1 gene. Notably, the Cdh1 promoter is insufficient to confer strict cell-type specificity, even when all known E-box components are present. On the other hand, E-cad's intron 2 shows up as a significant regulator of Cdh1 expression (Stemmler et al., 2005).

The most significant identifying feature of the transcriptional network specific to MET is the epithelial signature determining cellular homeostasis. When subjected to various signals during EMT-MET processes, it includes changing the cellular identity (Lamouille et al., 2014; Macara et al., 2014). The MET event can be exhibited by numerous signaling pathways, transcription factors, and epigenetic modifiers at various levels in cells, and these parameters may change depending on physiological and pathological situations (Lamouille et al., 2013). This relates to how EMT is unveiled. Recent studies (Polo and Hochedlinger, 2010) have identified MET as one of the initial processes in converting murine embryonic fibroblasts into Induced pluripotent stem cells (iPSCs). The MET process is essential for the production of induced pluripotent stem cells. This process is initiated by activating the Cdh1 promoter by Klf4, followed by the activation of Nanog, which will maintain the core pluripotency network.

Interestingly, an epithelial fate supports the initiation of MET, enhancing reprogramming efficiency. E-cad is crucial for maintaining embryonic stem cells in a pluripotent state (Redmer et al., 2011). Reduced E-cad expression during induced pluripotent stem cell generation interferes with the initiation of MET and diminishes somatic cell programming potential (Bedzhov et al., 2013). Apart from its role in embryogenesis morphogenetic events, MET also holds a critical function in the metastasis and colonization of tumor cells in distant regions (Bakir et al., 2020; Banyard and Bielenberg, 2015). Intertwining the

pluripotency network with EMT-MET events is essential for establishing metastatic foci. Earlier studies have also identified pluripotent-like states in certain cancer cells, like sarcoma and melanoma, induced through METmediated reprogramming
(Takaishi et al., 2016).

2.3 Transcriptional Regulation of EMT

The regulation of EMT involves many well-known factors, including coordinated changes in gene expression networks regulated by long noncoding RNAs (lncRNAs), microRNAs (miRNAs), and TFs. The interplay of these components governs the delicate equilibrium between epithelial and mesenchymal states, guiding cellular plasticity and morphological transitions. Among the pivotal contributors to EMT regulation are transcription factors such as Snail Family proteins—Snail1/2, as well as the Zinc finger E-box binding (Zeb) homeobox family proteins like Zeb1/2. Additionally, the TWIST family proteins, namely Twist1/2, join forces with these TFs to suppress epithelial markers such as E-cad, Claudin, Occludin, Mucin-1, and PTEN while concurrently activating mesenchymal markers like N-cadherin, Vimentin, and Vitronectin.

Numerous significant lncRNAs have been identified as contributors to the induction of EMT, and among them are highly upregulated in liver cancer (HULC), metastasis-associated lung adenocarcinoma transcript 1 (MALAT-1), H19, and HOX transcript antisense intergenic RNA (HOTAIR). For instance, heightened expression of HULC in gastric cancer correlates with advanced metastasis stages; intriguingly, silencing of HULC can effectively reverse the EMT phenotype. Similarly, MALAT-1 exhibits increased expression in primary tumors that metastasize, and its involvement is linked to the activation of Wnt signaling. H19's interaction with EZH2 also facilitates bladder cancer metastasis by inhibiting E-cadherin expression (Guo et al., 2014).

MicroRNAs significantly influence EMT regulation through their targeted interactions with specific ligands, receptors, and signaling pathways. A noteworthy case is miR-7, which suppresses Snail, enhances E-cad expression, and thereby offers a partial EMT reversal through targeting IGF1R. Furthermore, miRNAs like miR-206, miR-221, miR-222, miR-130a, miR-17, miR-92, and miR-145 promote EMT processes (Brabletz et al., 2011). Recent investigations have also uncovered miR-200's capacity to target Jagged1, resulting in ZEB1 downregulation (Guo et al., 2014; Saydam et al., 2009).

2.4 Transcriptional Regulation of MET

Although there have been numerous publications on the regulation of EMT, there are not many reports looking into the mechanisms underlying MET. Since it is thought that only EMT-inducing factors are responsible for the regulation of EMT, there are few publications investigating the mechanisms underlying MET regulation. However, studies conducted in recent years have revealed dynamic transcriptional changes during EMT-MET brings attention to factors such as Grhl2/3, Hnf4α and Ovol1/2 involved in the processes. In addition to transcription factors, several miRNAs have important roles in MET.

KLF4 (Krüppel-like factor) is a transcription factor containing zinc-finger protein at various intervals such as cell proliferation, differentiation, and proliferation. It has been shown that miR-103 and 107 cause metastases by directly targeting the DAPK (dead protein kinase) molecule (J. Chen et al., 2012), which calculates apoptosis in response to stimuli such as TGFβ.

Similarly, it has been suggested that miR-10b causes esophageal cancer metastases by targeting KLF4. Additionally, Hnf4α is associated with the EMT core regulator Snai1 in HCC cells by regulating the expression of miR-29a and miR-29b (Cicchini et al., 2015; Dubois et al., 2020). Dynamic transcriptional alteration during EMT-MET brings attention to elements implicated in the processes, such as Grhl2/3, Hnf4, and Ovol1/2 (Alotaibi et al., 2015; Roca et al., 2013).

2.4.1. Grhl3

Grainy head transcription factors are conserved factors that are involved in the regulation of epidermal barrier formation. It is known that Grhl3 expression is specific for tissue and development in many ectodermal and endodermal cell types in the developmental and adult skin (Gustavsson et al., 2008; Mlacki et al., 2015). Recent studies highlight the place of GRHL3 in skin squamous cell carcinoma, hepatocellular carcinoma, breast, gastric, colorectal, prostate, and cervical cancer (Frisch et al., 2017; Kotarba et al., 2020). It is thought that the preventive role of GRHL3 in breast cancer and its possible contribution to the tumor suppressor pathway is due to the fact that GRHL3 directly regulates E-cadherin. GRHL3 is not tumorogenic in the mammary gland, but it can positively affect the expression of E-cadherin throughout the MET process in various malignancies, including lung cancer (Alotaibi et al., 2015; Mlacki et al., 2015). On the other hand, recent findings show that Grhl3 can function as both an activator and a repressor. It demonstrates that Grhl3 might play diverse functions in controlling migration and invasion (Klein et al., 2017).

2.4.2. Hnf4α The hepatocyte differentiation factor Hnf4α is abundant in the liver, kidney, and intestine. The balance between its regulators and Hnf4α influences EMT-MET events (Cattin et al., 2009; Hatziapostolou et al., 2011; B. D. Moore et al., 2016). Hnf4α has been associated with the initiation of MET (Alotaibi et al., 2015). It causes MET-like phenotypic changes by modulating the epithelial infrastructure and suppressing the mesenchymal program. It is responsible for the metastatic function of HCC cells and regulates the balance between epithelial and mesenchymal states (Yao et al., 2013). In addition, the Grhl3/Hnf4α interaction is responsible for stabilizing the epithelial infrastructure through suppression of the mesenchymal program. Our previous studies revealed that Grhl3 contributes to the regulation of Hnf4α during MET in NMuMG cells (Alotaibi et al., 2015).

2.4.3. Elf3

Ets transcription factors are one of the transcription factor families that are expressed both ubiquitously and in a tissue-specific manner; it is the largest family in humans, consisting of about 30 members. Ets transcription factors bind to a typical 5'-GGA(A/T)-3 DNA sequence and are characterized by conserved DNA binding domains (Andreoli et al., 1997; Cooper et al., 2014; Hollenhorst et al., 2011). Members of this family are also MAP kinases, Erk1/2, p38, and JNK, and they can act as up and down effectors of most signaling pathways, including trans-acting phosphoproteins (Otero et al., 2012). Therefore, EMT and MET have important roles in many biological processes, such as differentiation, development, proliferation, apoptosis, and tissue remodeling (Maroulakou and Bowe, 2000; Wasylyk et al., 1993).

Elf3 is one of the main Ets transcription factors expressed in tissues rich in the epithelium, such as the pancreas , colon, kidney, mammary gland, and skin (Oliver et al., 2012). Our EMT/MET model shows that the expression of Elf3 in NMuMG cells is stable during EMT and MET, in contrast to Cdh1 (and other epithelial transcription factors) (Sengez et al., 2019). This indicates other functions of Elf3 in mesenchymal cells, which could be distinct from those in epithelial cells. Similarly, other studies show that Elf3 can also be expressed in nonepithelial cells and induced by the proinflammatory cytokines TNF-α, and IL-1β (Oliver et al., 2012; Otero et al., 2012).

ELF3 is critical in epithelial cell differentiation, gut development, inflammation, and apoptosis. In addition to its roles in cancer epithelium, as in breast, lung, and prostate cancers, It is known to be necessary for the pathophysiology of cells (Gajulapalli et al., 2016; Tymms et al., 1997). It has been shown that ELF3 activates both epithelial cells of Type II TGFβ receptor gene (TGFβR-II) and binds to the TGFβR-II promoter in vivo (Kopp et al., 2004). For example, ELF3 controls differentiation of intestinal epithelial by changing TGFβR-II expression pattern during development. With GRHL3, the transcriptional regulator ELF3 has been linked to human urothelial cytodifferentiation. Elf3 also plays a role in the expected localization of Ecadherin at the plasma membrane, which is essential during the progression of MET. Again, in the MET process, It can regulate the expression of Grhl3 by binding to conserved regions on the Grhl3 promoter. Loss of Elf3 expression in the cell interferes with the initiation of MET and causes it to remain in a mesenchymal-like state (Figure 1) (Sengez et al., 2019). Taken together, we can hypothesize that Grhl3 and Elf3 are part of a positive feedback network.

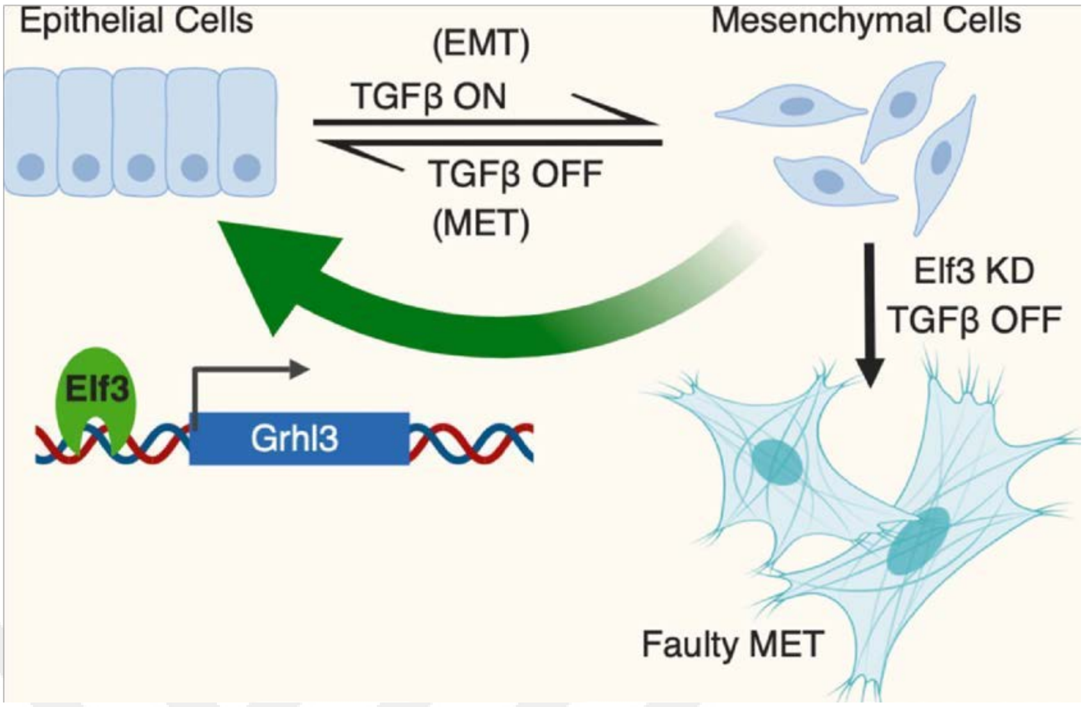

Figure 1. Illustration of EMT and MET by showing the effect of Elf3 knockdown. Upon exposure to TGFβ, cells undergo EMT lose their cell-cell adhesion. Upon removal of TGFβ from the culture medium, these cells transition back to the epithelial state via MET. However, Elf3 knockdown results in impaired MET, possibly due to Grhl3 Elf3 interaction.

2.5. Epigenetic Regulation of EMT/MET

Since epigenetic modifications can affect gene activity and gene expression independently of DNA sequence and are reversible, it is important in many biological processes. DNA methylation involves the methylation of cytosines (C) in CpG regions, a site where C lies next to guanine (G) in the DNA sequence, leading to the repression of transcription. Histone modifications and post-translational modifications, which alter proteins in an enzymedependent way, also form a significant portion of the epigenetic control. Because processes that require the entire DNA template (transcription, replication, recombination) are affected by the complex structure of the chromatin infrastructure. Depending on the cell's pathophysiological environment, DNA methylation, histone post-translational modifications, and non-coding RNA production can all be reversed. Additionally, epigenetic changes have been strongly associated with the control of EMT and have been proposed to confer the required plasticity to control the aggressiveness, invasion, and metastasis of cancer (Chaffer et al., 2016).

MacroH2A1 (mH2A1) has a particular function in regulating EMT and the reprogramming capacity of cellular conditions (Hodge et al., 2018). It has also been shown that mH2A1 inhibits reprogramming and maintains cell identity by keeping cells in the MET state (Pliatska et al., 2018). In addition, H2A.Z acts as a key factor in the regulation of EMT (Domaschenz et al., 2017).

In some cancer types, the absence of the H2A.X histone variation, which is crucial for DNA repair and genome integrity, initiates EMT (Weyemi et al., 2016). Although global changes in DNA methylation and histone modifications are key events between epigenetic mechanisms, the conservation of repetitive elements significantly impacts regulatory changes and genome stability.

2. MATERIALS AND METHODS

3.1. Type of Study

It is an experimental study supported by in-silico experiments.

3.2. Time and Place of Study

The study was conducted at Izmir Biomedicine and Genome Institute between December 2021 and August 2023.

3.3. Materials of Study

The experiments utilized the Normal Murine Mammary Gland cell line (NMuMG), procured from ATCC (ATCC® CRL-1636) in 2017. This cell line is a widely recognized and frequently employed model for studying EMT and MET (Miettinen et al., 1994). This model is favored due to its distinct gene signature alterations manifested in observable morphological changes. Upon exposure to TGFβ, these cells undergo EMT labeled as TGFβ3, characterized by the downregulation of Cdh1, the rearrangement of cortical actin to stress fibers, and the upregulation of mesenchymal genes such as N-cadherin and Vimentin. Notably, upon removal of TGFβ from the culture medium, these cells transition back to the epithelial state via MET within 72 hours labeled as PT72 (posttransition) (Alotaibi et al., 2015) (Figure 2.).

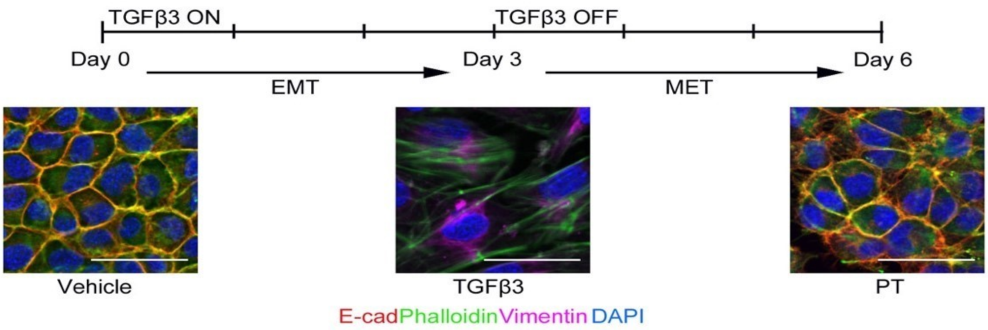

Figure 2. The EMT-MET processes were visualized using immunofluorescent staining. At Day 0 (Vehicle), epithelial NMuMG cells were observed with the epithelial marker E-cad (red) prominently present in the cell membrane, along with actin staining by phalloidin (green). Following a 72-hour treatment with TGFβ on Day 3 (TGFβ3), the cells exhibited a mesenchymal phenotype, with the mesenchymal marker vimentin appearing in purple around the nuclei. Notably, the epithelial marker E-cad was no longer visible. Upon removing TGFβ from the medium, the cells were cultured in a regular medium for 72 hours under Post-treatment (PT) conditions. Interestingly, these cells reverted to the epithelial state, as evidenced by the reappearance of the epithelial marker E-cad (red) in the cell membrane, similar to the pattern observed in the initial Vehicle state.

3.3.1 Cell Culture Materials, Reagents & Cell Lines

Table 1. Cell culture reagents

Materials	Cat. No	Vendor
DMEM, high glucose	41965039	Gibco
Trypsin-EDTA (0.25%), phenol red	25-200-056	Gibco
DPBS, no calcium, no magnesium	14190094	Gibco
Fetal Bovine Serum, qualified, Brazil	10270106	Gibco
MEM Non-Essential Amino Acids Solution (100X)	11140035	Gibco
Sodium pyruvate 100 mM	p04-43100	PAN-Biotech
Penicillin-Streptomycin (10,000 U/mL)	15140122	Gibco
FuGENE® HD Transfection Reagent	E2311	Promega
Lipofectamine™ RNAiMAX Transfection Reagent	13778150	Invitrogen
DMSO	A3672,0100	Applichem
pRL-TK		Promega

3.3.2 PCR, cDNA, and qPCR Reagents

Table 2. PCR, cDNA, and qPCR Reagents

Materials	Cat. No	Vendor
Taq DNA Polymerase with Standard Taq (Mg-free) Buffer	M0320S	NEB
Q5® High-Fidelity DNA Polymerase	M0491L	NEB
Phusion™ High-Fidelity DNA Polymerase	F-530XL	Thermo Scientific
Deoxynucleotide (dNTP) Solution Mix	N0447S	NEB
T4 DNA Ligase	M0202S	NEB
AMPIGENE® qPCR Probe Mix NoROX	ENZ-NUC1071000	ENZO
MicroAmp™ Fast Optical 96-Well Reaction Plate with Barcode, 0.1 mL	4346906	Applied Biosystems
MicroAmp™ Optical Adhesive Film	4360954	Applied Biosystems
Universal Probe Library probes		Roche

3.3.3 siRNA Sequence Information

Table 3. siRNA Sequence

siRNA	Sequence	Vendor
Elf3	TTGAACCAACTTGTTCGATAA	Qiagen

3.3.4 Immunofluorescence Labelling Reagents

Table 4. Immunofluorescence Labelling Reagents

Materials	Cat. No	Vendor
Formaldehyde	F8775	Sigma
Triton X-100	T8787	Sigma
E-cadherin antibody	610181	BD
DAPI	D1306	Invitrogen
Alexa Fluor 488 Phalloidin	A12379	Invitrogen
Prolong Diamond Antifade Mountant solution	P36962	Thermo Fisher Scientific

3.3.5 Plasmid Construction

Dmnt1, Uhrf1, and Dnmt3b promoters were cloned into the luciferase reporter vector pGL4.10 (Promega).

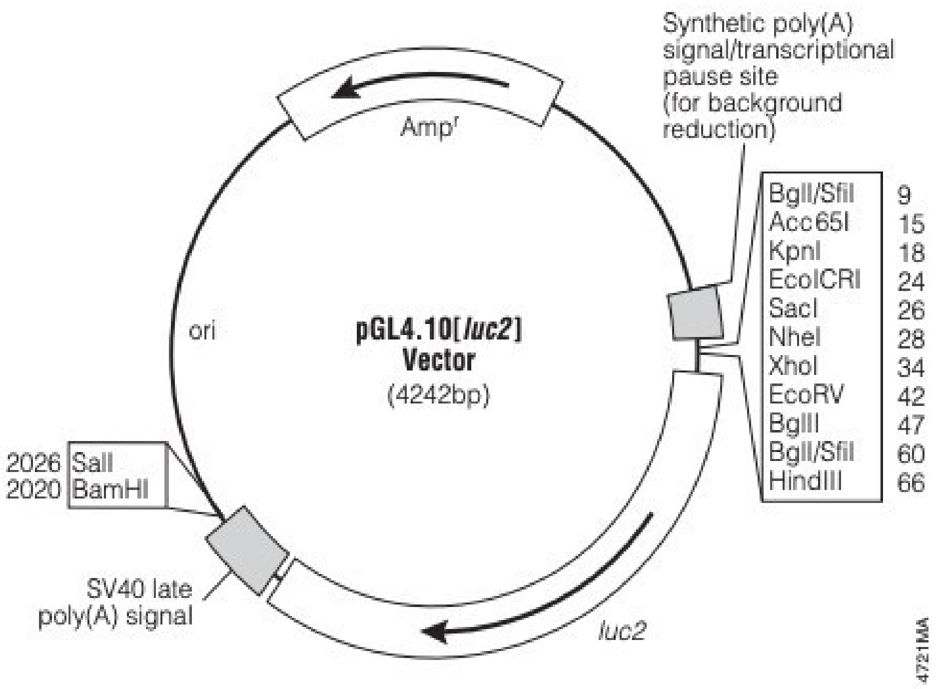

Figure 3. pGL4.10 plasmid construction.

The Elf3 expression vector was prepared by cloning the coding sequence of the mouse Elf3 in the mammalian expression vector pcDNA4_TO_Myc-His A (Invitrogen).

3.3.6 Molecular Cloning Reagents

Table 5. Molecular Cloning Reagents

Materials	Cat. No	Vendor
Q5® High-Fidelity DNA Polymerase	M0491L	NEB
Terra PCR Direct Polymerase Mix	639270	Takara
Deoxynucleotide (dNTP) Solution Mix	N0447S	NEB
HindIII-HF	R3104S	NEB
XhoI	R0146S	NEB
KpnI-HF	R3142S	NEB
SacI	R3156S	NEB
NheI-HF	R3131S	NEB
BglII-HF	R0144S	NEB
T4 DNA Ligase	M0202S	NEB

3.3.7 Bacterial Reagents

Table 6. Bacterial Reagents

Materials	Cat. No	Vendor
Ampicillin Sodium Salt BioChemica	A0839,0010	AppliChem
Yeast Extract	Y1625-250G	Sigma
Agar	05039-50G	Sigma
Tryptone BioChemica	1553.0500	AppliChem
NaCl	1.06404.1000	Merck
NucleoBond Xtra Maxi kit	740414.10	Macherey-Nagel

3.3.8 ChIP Reagents

Table 7. ChIP Reagents

Materials	Cat. No	Vendor
Formaldehyde	F8775	Sigma
Glycine	CE.453807	Carlo Erba
UltraPure Salmon Sperm DNA Solution	15632011	Thermo Scientific
Bovine Serum Albumin	GE17-0780-01	Cytiva
Proteinase K	P8107S	NEB
RNaseA	A2760.0100	Applichem
ELF3/ESE-1 antibody	NBP1-30873	Novus
Rabbit control IgG	2729S	Cell Signaling
Chelex	142-1253	BİORAD
SDS	817034100	Merck
EDTA	60-00-4	Sigma
Trizma base	T1503-1KG	Sigma

Protease Inhibitor Cocktail	04693116001	Roche
NaCl	M106404.100	Merck
Triton X-100	T8787	Sigma
NP-40	A1694.0500	Applichem
sodium deoxycholate	30970	Sigma
LiCl	L9650	Sigma
Protein A-Sepharose® CL-4B	GE17-0780-01	Cytiva

3.3.9 Methylated DNA Immunoprecipitation- hydroxymethylated DNA

Immunoprecipitation (MeDIP-hMeDIP) Reagents

Table 8. meDIP and hmeDIP Reagents

Materials	Cat. No	Vendor
Sodium phosphate	342483	Sigma
NaCl	M106404.100	Merck
Triton X-100	T8787	Sigma
UltraPure™ Salmon Sperm DNA Solution	15632011	Thermo Scientific
BSA	GE17-0780-01	Cytiva
Proteinase K	P8107S	NEB
RNaseA	A2760.0100	
5-Methylcytosine (5-mC) antibody (mAb)	61480	Active motif
5-Hydroxymethylcytosine (5-hmC) antibody (pAb)	39770	Active motif
rabbit control IgG	2729S	Cell Signaling
Trizma base	T1503-1KG	Sigma
Protease Inhibitor Cocktail	04693116001	Roche

3.3.10 Other Chemicals, Consumables, and Commercial Kits

Materials	Cat. No	
NucleoSpin RNA kit	740955.50	Macherey-Nagel
NucleoSpin Gel and PCR Clean-up kit	740609.50	Macherey-Nagel
Quick-DNA Miniprep Plus kit	D4069	Zymo
Dual-Glo® Luciferase Assay System	E2940	Promega
GeneRuler 1 kb DNA Ladder	SM0313	Thermo Scientific
GeneRuler 50 bp DNA Ladder	SM0372	Thermo Scientific
Agarose	A9536-500G	Sigma
Absolute Ethanol	9.200.262.500	Isolab
Ultrapure DNAse/RNAse free dH2O	10977035	Thermo Scientific

Safe View	G108	ABM
Boric acid	10043-35-[1]	Merck
EDTA	E5134-500G	Sigma
Recombinant Human TGFβ3	100-36E-10UG	PEPROTECH
		Vendor

Table 9. Other Chemicals, Consumables, and Commercial kits

Table 10. Hardware and machines used in this study

Machine	**vendor**
pH Meter	HANNA Instruments
Toploader Balance 820 g x 0.01g	Sartorius
SimpliAmp™ Thermal Cycler	Applied Biosystems
Owl™ EasyCast™ B1A Mini Gel Electrophoresis	ThermoFisher Scientific
Microwave oven	Beko
mySPIN™ 6 Mini Benchtop Centrifuge	ThermoFisher Scientific
Vortex Mixer	ThermoFisher Scientific
Hotplate Stirrer Thermolyne	ThermoFisher Scientific
Waterbath	Nuve
Centrifuge 5810R	Eppendorf
Centrifuge MicroCL 17R	ThermoFisher Scientific
Incubator MaxQ 4000	ThermoFisher Scientific
ABI 7500 Fast Thermal Cycler	ThermoFisher Scientific
NanoDrop 2000	ThermoFisher Scientific
Centro Microplate Luminometer XS3 LB960	Berthold technologies
Gel Doc XR+ System with Image Lab Software	Bio-Rad
Confocal Microscopy	Zeiss LSM880
S220 focused-ultrasonicator	Covaris
Bioruptor Pico Sonication device	Diagenode

3.3.12 Chemical Recipes

LB Broth (1L)

10 g Tryptone
5 g Yeast extract
5 g Sodium Chloride **LB**

Agar (1L)

1 L LB broth
15 g Agar **10X TBE**
(1L)

108 g Tris

[1] ***.3.11 Hardware & Machines***

55 g Boric acid
40 ml 0.5 M pH:8 EDTA

1% Agarose Gel

0.5 g Agar
50 mL 0.5X TBE

ChIP Lysis Buffer (50 mL)

5 mL 10% SDS (1% Final Conc.)
1 mL 500 mM EDTA (10 mM Final Conc.)
2.5 mL 1M Tris (pH 8.0) (50 mM Final Conc.) +
Protease Inhibitor Cocktail **ChIP Dilution Solution (250 mL)**

250 µl 10% SDS (0.01% Final Conc.)
27.5 mL 10% Triton X-100 (1.1% Final Conc.) 600 µl 500 mM EDTA (1.2 mM Final Conc.) 4.175 mL Tris (pH 8.0) (16.7 mM Final Conc.) 8.35 mL 5M NaCl (167 mM Final Conc.) + Protease Inhibitor Cocktail **Wash Buffer 1 (250 mL)**

2.5 mL 10% SDS (0.1 % Final Conc.)
25 mL 10% Triton X-100 (1% Final Conc.)
1 mL 500 mM EDTA (2 mM Final Conc.)
5 mL 1M Tris (pH 8.0) (20 mM Final Conc.)
7.5 mL 5M NaCl (150 mM Final Conc.) **Wash Buffer 2 (250 mL)**

2.5 mL 10% SDS (0.1 % Final Conc.)
25 mL 10% Triton X-100 (1% Final Conc.)
1 mL 500 mM EDTA (2 mM Final Conc.) 5 mL 1M Tris (pH 8.0) (20 mM Final Conc.) 25 mL 5M NaCl (500 mM Final Conc.) **Wash Buffer 3 (250 mL)**

0.5 mL 500 mM EDTA (1 mM Final Conc.)

2.5 mL 1M Tris (pH 8.0) (10 mM Final Conc.)

25 mL 10% NP-40 (1% Final Conc.))
2.5 g sodium deoxycholate (1% Final Conc.)

7.8125 mL 8M LiCl (0.25M Final Conc.) **Wash Buffer**

4 (250 mL)

2.5 mL 1M Tris (pH 8.0) (10 mM Final Conc.)
0.5 mL 500 mM EDTA (1 mM Final Conc.)

10% Chelex (50 mL)

5 g Chelex
Bring volume to 50 ml with sterile ddH_2O

10× IP buffer

100 mM Na-Phosphate, pH 7.0
1.4 M NaCl
0.5% Triton X-100

3.4. Variables of Study

The time points of the NMuMG cell model of EMT and MET are independent variables. The expression values of identified transcripts are dependent variables. Dependent variables include the siRNAs used in silencing research, the binding sites of Elf3 identified, and the GEO databases, which include sequence-based information on curated, publicly available gene expression profiles. Promoter methylation and hydroxymethylation levels are dependent variables in all EMT-MET and MET in the absence of Elf3.

3.5. Tools For Data Collection

All data collection and processing operations were conducted on an Apple MacBook Air, 8 GB RAM computer with MacOS Monterey 12.6.3 operating system, and IBG HPC environments have been used for data collection in this study.

3.6 Study Plan and Calendar

Dec- Nov 21	Read processing, alignment, expression quantification
Jan- Feb 22	Differential expression analysis, enrichment analysis, visualization
March-April 22	Conservation analysis of promoters and molecular cloning
May- Aug 22	Promoter transfection, EMT-MET induction validation
Sep-Nov 22	siElf3 transfection and validation

Dec-May 23	MeDIP, hMeDIP, ChIP experiments, and validations
June-Aug 23	Writing

3.7 Data Evaluation

3.7.1 Cell Culture and EMT/MET Experiment Model

NMuMG cells were cultured in DMEM supplemented with 10% fetal bovine serum, 1X MEM NEAA, 1% penicillin/streptomycin, and Sodium pyruvate. NMuMG cells were grown in a humid environment with 10% CO_2 at 37 °C. For EMT induction, NMuMG cells were incubated in a complete medium supplemented with 2.5 ng/mL TGFβ3 for 72 h (labeled as TGFβ3). The MET induction was initiated by TGFβ3 withdrawal, washing the plates three times with PBS, and incubating for an additional 72 h in fresh complete medium (labeled PT as in Post-treatment). NMuMG cells used as control were labeled as Vehicle.

3.7.2 siRNA Knockdown and mRNA Expression Analysis

siRNAs against Elf3 were purchased from Qiagen for siElf3_2; the sequence is: TTGAACCAACTTGTTCGATAA. NMuMG cells were transfected with 50 nM siRNA using the Lipofectamine RNAi Max as recommended by the manufacturer and collected 72 h later. Total RNA was isolated from treated and control cells using the Nucleospin RNA II kit. Concentrations of samples were measured using the instrument NanoDrop 2000. 1 µg RNA was converted to cDNA using the Maxima First Strand cDNA Synthesis Kit. cDNA was then diluted 1:10 and used for qPCR. AMPIGENE qPCR probe mix (Enzo) and Universal Probe Library probes were used for the experiment as recommended by the manufacturer. Analysis and quantification of qPCR were performed using the ΔΔCt method. ***3.7.3 RNA-seq Data Analysis***

3.7.3.1 Raw Data Processing

Quality control of four FASTQ formatted files with sequence information underwent a quality check with FastQC tool (version 0.11.9) to detect if samples contain low-quality reads or adapter sequences. To avoid adaptor contamination, trimmomatic software (version 0.39) was used to remove adaptors. After trimming, clean reads were detected in the quality control stage and proceeded to further analysis. Read alignment was performed with HISAT2 (version 2.1.0). Genome Reference Consortium Mouse Build 38 (GRCm38) release M21 provided by the GENCODE Project was selected as a reference genome. A custom version of these builds was used to create a genome index in HISAT2 hisat2-build -p command. In the alignment step, the hisat2 -p --dta x -U -S command was used to align sequences to reference genome with resulting output files large SAM (Sequence Alignment Map). For the next step, the SAM file is converted to a Binary Alignment Map (BAM) file by using samtools (version 1.15.0) to sort by chromosomal coordinates with the following command: -@ <n_threads> -o <BAM> <SAM>. To quantify genes, the R statistical computing environment (version 4.1.1) was used with the required package, Rsubread (version 2.8.2). Using the featureCounts() function in the Rsubread package, exonic region counts are detected in each BAM file. As external annotation input, a custom GTF file was used. By using the rpkm() function of another R package “edgeR” (version 3.42.2), quantified transcripts RPKM values together with raw counts were obtained.

3.7.3.2 Differential Expression Analysis

In order to define the differences in the expressions of protein-coding and non-coding genes between scrambled and Elf3 knock-down samples, differential expression analysis was carried out. TMM normalization, dispersion estimation, and exact test between groups was performed with EdgeR.

3.7.3.3 Visualizations

All visualizations were performed on R, using packages ggplot2, ggpubr, EnhancedVolcano.

3.7.4 Immunofluorescence Labeling and Confocal Microscopy

Cells were washed with PBS before being fixed for 10 minutes at room temperature with 4% formaldehyde. After that, it was permeabilized with 0.25% Triton X-100 for 10 minutes and rinsed three times with PBS. After washing three times with PBS, cells were incubated with E-cadherin antibody with 5% BSA (1:200) for one hour at room temperature in the dark. Then, samples were washed three times with PBS and incubated with Alexa Fluor 488 Phalloidin for one hour at room temperature in the dark. Nuclei were visualized with DAPI. Prolong Diamond Antifade Mountant solution was used to mount slides. Confocal microscopy was performed using an LSM 880 microscope and ZEN software.

3.7.5. Conservation Analysis

The UCSC Genome Browser database was used to get the promoter sequences of interest in FASTA format. These sequences were scanned with the 'CLC Sequence Viewer' to reveal the promoter components. Then, using the mVista and ConTra v3 program, 1-1.5 kb promoter regions of several species were compared. We identified potential transcription factor binding locations using the "JASPAR" database.

3.7.6 Construction of Reporter Vector Sequences

Dnmt1, Uhrf1, and Dnmt3b promoters were cloned into pGL4.10 vector (Promega) to investigate the effect of Elf3 transcription factor on promoter activity of Dnmt1, Uhrf1 and Dnmt3b genes. The promoter region (1-1.5kb) was amplified using mouse genomic DNA, and different restriction enzymes cut-off regions were created for each gene. To amplify Dnmt1 and Uhrf1 promoters, Q5 polymerase was used. Reaction performed in 50 µL volume containing 10 µL 5x buffer, 200 µM dNTP, 10 pmol of each primer (see appendix table.13), 0.5 µL Q5 polymerase, 200ng NMuMG genomic DNA. Thermal cycler conditions were an initial denaturation step at 98 °C for 30 s, 30 cycles of 98 °C for 10 s, 60 °C for 15 s, and 72 °C for 1 m, followed by a final extension at 72 °C for 5 min. Dnmt3b was amplified with Takara Polymerase in a 10 µL reaction volume that containing 5 µL 2X terra buffer, 3 pmol of each primer (appendix 1 table 13.), 5% DMSO, 0.2 uL Terra polymerase, and 50 ng NMuMG genomic DNA. Thermal cycler conditions were an initial denaturation step at 98 °C for 2 m, 40 cycles of 98 °C for 10 s, 68 °C for 1.5 m. The amplified fragment after enzymatic cleavage were inserted into the pGL4.10 vector; the resulting clones were sequenced for conformation. The promoter activity of cloned genes was analyzed by the DualGlo Luciferase Test System. Additionally, to identify the minimal promoter region and Elf3 transcription factor dependent activity of cloned genes expression was analyzed.

3.7.7 Luciferase Reporter Activity Measurement

NMuMG cells grown in a 48-well cell culture dish were transfected with the plasmid DNA “Fugene HD” using the transfection reagent while the cells were suspended. Transfection experiments were performed with 100ng DNA containing 2.5ng pRL-TK to standardize the transfection efficiency. Firefly luciferase reporter values of cells transfected with expression plasmid or empty vector were measured using a luminometer and normalized to the values of the control Renilla luciferase. The fold change was calculated by proportioning the values of the empty vector.

3.7.8 Chromatin Immunoprecipitation (ChIP)

ChIP was administered to a healthy cell undergoing EMT and 48 hours of MET, as described previously, with minor modifications (Alotaibi et al., 2010). NMuMG cells were grown and treated in 10 cm plates. Following 10 min crosslinking with formaldehyde (final concentration is 1%) and 10 min quenching with glycine (final concentration is 0.125 M), cells were washed three times with PBS, and cells were scraped off in DMEM. Pellets obtained after 5 minutes of centrifugation at 3000 g were lysed in 1 ml cell lysis buffer. 50 µl of unsonicated DNA from the cell lysate was taken into a separate tube as a control. Cell lysates were then sonicated in the S220 focusedultrasonicator for 30 min (60 s on/60 s off; Peak Power: 140 W; Duty factor: 15; Cycles/burst: 200; water temperature: 4 °C). Chromatin shearing was tested by agarose gel electrophoresis. The samples obtained in the desired fragment range were subjected to dilution with ChIP dilution solution (1:10). Immunoprecipitation was then performed at 4 °C for 16 h using an antibody against ELF3/ESE-1, and a rabbit control IgG in a rotator with 12 rpm. 50 µl Protein A (50% slurry) preabsorbed with salmon sperm DNA (and washed with dilution buffer) were added and incubated with tumbling at 4 °C for 2 hours in a rotator with 12 rpm. Immunoprecipitations were centrifuged for 2 minutes at 3000 g, and supernatants were carefully removed. Pellets were then washed with 4 different wash buffers (wash buffers 1-4) and centrifuged after each wash. The removed supernatant was then purified using 10% Chelex. To reverse the cross-linking of the DNA and proteins, samples were incubated for 10 minutes at 95 °C and subjected to Proteinase K (30 min at 95 °C) and RNaseA incubation (15 min at 37 °C). Quantitative real-time PCR was performed using the TaqMan Universal master mix II and Universal Probe Library probes. Amplification was done using the primers and probes shown in Appendix 1 in the ABI PRISM 7500 Fast qPCR System (Table 14.) at 95 °C for 5 min, 55 cycles of 95 °C for 15 s and 60 °C for 1 min. Data

3.7.9 Methylated DNA Immunoprecipitation and hydroxymethylated DNA Immunoprecipitation (MeDIP-hMeDIP)

DNA immunoprecipitation (DIP) method was applied with DNA collected from healthy EMT and MET cells, followed by DNA methylation and hydroxymethylation studies. The resulting DNA (2 µg) was sonicated using the Bioruptor Pico Sonication device, 30/90; 4/4 cycle sonication. Comparing DNA and gDNA with the gel electrophoresis method and applying sonication between 200-1000 bp fragmentation was observed. After the method was observed to be successful, the obtained sonicated DNAs were denatured with 95°C Heat Block for 10 minutes and immediately placed on ice to prevent rebinding. Denatured DNAs, which were kept on ice for 5 minutes, were taken into 1.5 µl microcentrifuge tubes and diluted by adding 900 µl of 1× IP buffer (10× IP buffer: 100 mM Na-Phosphate, pH 7.0, 1.4 M NaCl, 0.5% Triton X100). One sonicated and diluted DNA was used for each antibody. Three antibodies were used for each Vehicle cell, TGFβ3 cell, PT-Elf3 knockdown cell, and PT cell. Antibody amounts were calculated and added to match 2µg DNA. It was kept on the rotator device for 16 hours. 40 µl of Protein A sepharose beads were added to each and incubated with a rotator for 2 hours. After this step, immunocomplexes collected with protein A beads were washed 3 times with IP buffer and 1 time with TE Buffer. It was incubated at 95°C Heat Block by adding 10% Chelex, then at 55°C Heat Block by adding Proteinase K. In order to denature Proteinase K, it was again incubated in a 95°C Heat Block and centrifuged at 2000 rpm /1 min. The supernatant was separated and carefully transferred to the purification column, and the DNA was purified by centrifugation.

3.8. Limitation of the Study

No limitations are to be reported.

3.9. Ethics Committee Approval

This study was approved by the IBG local ethics committee with ethics protocol number 2023-013.

4. RESULTS

4.1. Elf3 Silencing Alters MET

4.1.1. mRNA Expression Analysis in Response to Elf3 Silencing

The NMuMG cell line serves as a well-established murine model for investigating the processes of EMT and MET. The EMT induction begins with

a three-day treatment of NMuMG cells with TGFβ3. This treatment leads the cells to acquire a mesenchymal phenotype. On the other hand, the induction of

MET can be initiated by the withdrawal of TGFβ3, the cells transition back to an epithelial phenotype after three days. Quantitative Polymerase Chain Reaction (qPCR) is utilized to evaluate the expression levels of marker genes associated with both epithelial and mesenchymal states. Assessing gene

expression levels of epithelial markers such as Cdh1, Hnf4α, Cebpα, Ovol2, and Grhl3 demonstrates a significant decrease during the EMT process, followed by recovery during MET (as shown in Figure 4). Conversely, a relatively consistent expression pattern is observed when examining the expression pattern of Elf3 in NMuMG cells throughout the EMT-MET progression.

For mesenchymal genes, the anticipated pattern suggests an increased gene expression during the mesenchymal state, accompanied by low levels during the epithelial state. This trend is mirrored in the expressions of Cdh2, Snai1/2, Zeb1/2, and Vim during the EMT/MET stages (Figure 5).

A B C

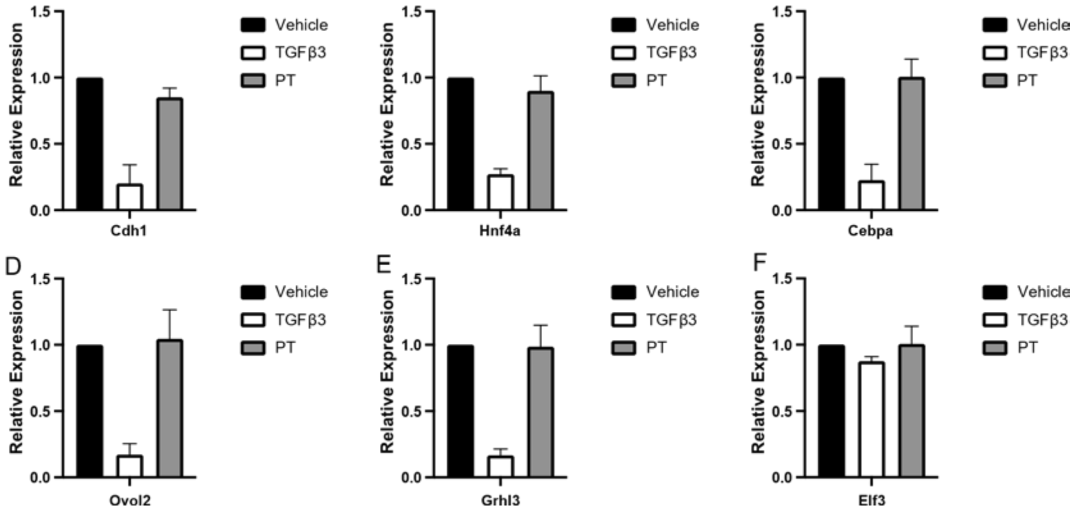

Figure 4. The expression levels of Epithelial genes during EMT-MET. The mRNA expression levels of Elf3 (F) are relatively stable in comparison to other epithelial genes: Cdh1 (A), Hnf4a (B), Cebpa (C), Ovol2 (D), Grhl3 (E) during the course of EMT/MET in NMuMG cells.

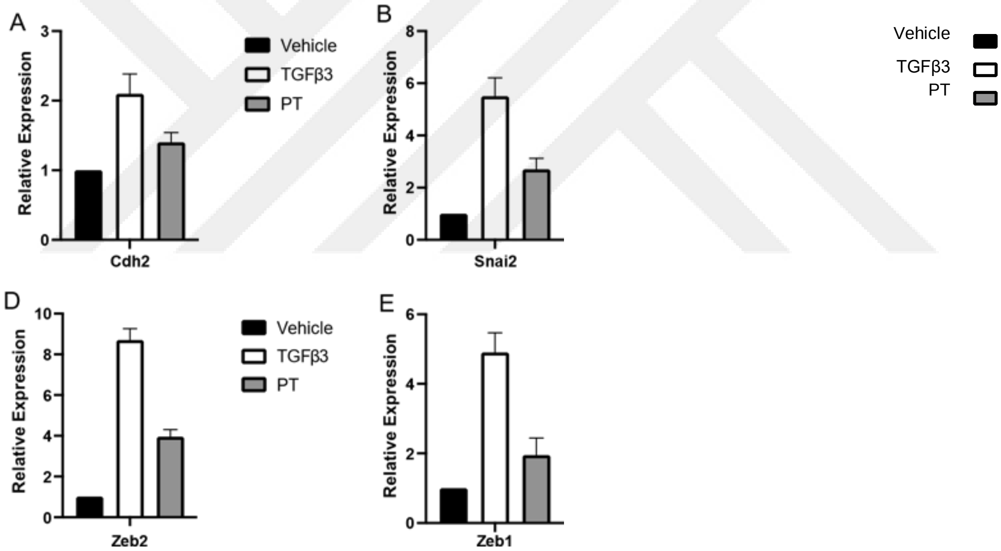

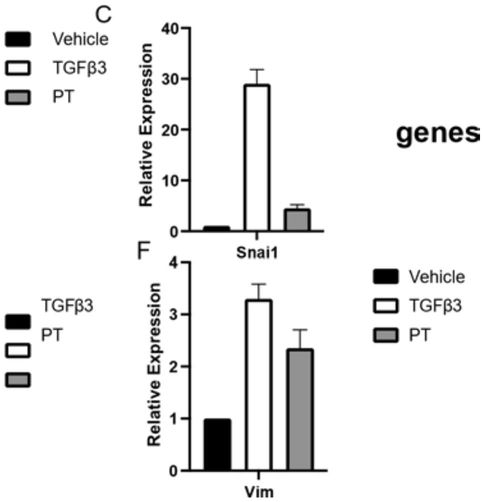

Figure 5. The expression levels of Mesenchymal genes during EMT-MET. The mRNA expression levels of Mesenchymal genes are upregulated during EMT and downregulated during the course of MET.

siRNA molecules were used to silence Elf3 expression at the initiation of MET in NMuMG cells. Subsequently, the expression level of Elf3 was quantified through qPCR, as depicted in the provided Figure. Notably, the transfection of Elf3-targeting siRNAs led to an effective knockdown of Elf3 in the transfected cells. Upon siElf3 silencing, a distinct phenomenon emerged: the cells exhibited an inability to initiate MET and displayed an enlarged and flattened morphology, as evident from confocal images (Figure 6). These aberrant cells were characterized by their oversized appearance, stress fibers, and the absence of E-cadherin expression on the plasma membrane. These collective findings point towards a compromised MET process, suggesting that the observed irregularity in MET could be attributed, at least in part, to the deficiency of E-cadherin on the plasma membrane, among other functions governed by Elf3.

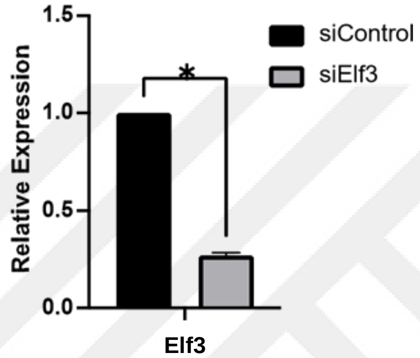

Figure 6. The siRNA-mediated silencing of Elf3. The efficiency of gene silencing was measured by qPCR analysis.

4.1.2. Immunofluorescence Labeling and Confocal Microscopy

The changes in gene expression in response to Elf3 silencing were also reflected by clearly visible morphological alterations. The Elf3 depleted cells were significantly enlarged, multinucleated, and showed cytosolic localization of E-cad, which is accompanied by cytoskeletal rearrangements (Figure 7). Our results were in agreement to our previous study, which investigated the role of Elf3 in the regulation of Grhl3 during MET (Sengez et al., 2019).

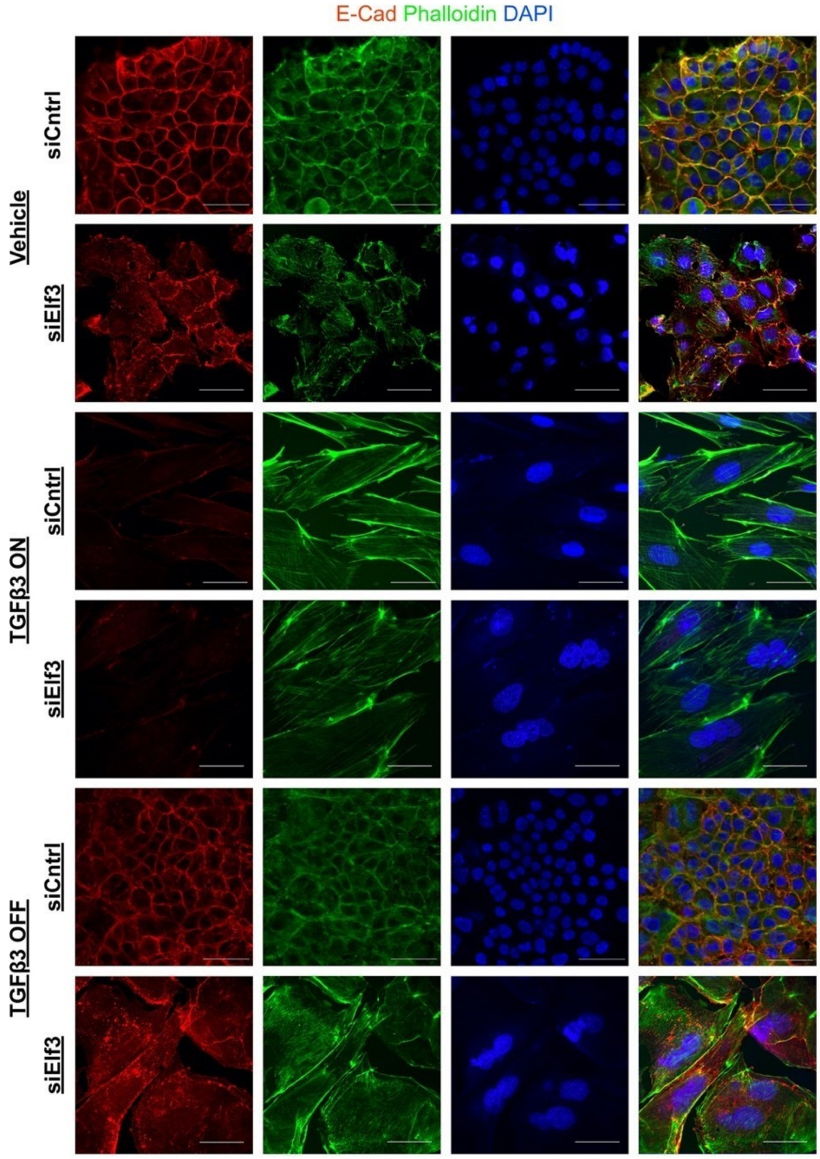

Figure 7. The siRNA-mediated silencing of Elf3 the immunofluorescence staining of NMuMG cells in EMT-MET. Confocal images demonstrate how TGFβ3 administration, withdrawal, and the silencing of Elf3 alter E-cadherin and Actin expression and intracellular distribution. E-cadherin (red) and actin distribution (Phalloidin, green) are displayed. DAPI (blue) is used to identify nuclei: scale bar, 50 μm.

4.2. RNA-seq Data Analysis

In order to understand the impact of Elf3 silencing on gene expression profiles during MET, NMuMG cells were transfected with siRNAs targeting Elf3 or nontargeting control siRNAs at the onset of MET. The cells were incubated for three days to allow the progression of MET. Then the cells were collected for RNA isolation. Total RNA was used for the preparation of NGS libraries, which were then analyzed using the Illumina platform (outsourced). The raw data was submitted to the NCBI SRA database under the accession number PRJNA693989.

4.2.1. Preprocessing and Alignment of Sequencing Reads

Raw data FASTQ files with PRJNA693989 BioProject accession number were downloaded and underwent quality check with FastQC tool to detect if samples contain low quality reads or any adapter sequences. Then, to remove adaptor sequences and low-qualified reads, trimmomatic software (version 0.39) had used. Following this refinement process, the qualitycontrolled reads were deemed suitable for subsequent analyses. HISAT2 was leveraged to align the reads against the Y chromosome-masked mm10 genome. This alignment endeavor yielded noteworthy statistics, as documented in the provided table. Impressively, each sample exhibited a robust overall alignment rate exceeding 95.4%. Table 11 shows the overall alignment scores for each sample.

Table 11. Alignment statistics of siCntrl and siElf3 samples for each replicate.

Samples	siCntrl		siElf3	
Replicates	1	2	1	2
Total Read Count	65472384	67761589	58786656	58759433
Overall Alignment Rate (%)	94.88	94.81	94.71	94.62

Gene expression insights were gained by utilizing the power of Principal Component Analysis (PCA) in illuminating sample correlations. The PCA plot effectively portrayed distinct patterns: "siCntrl" replicates exhibited notable dispersion, indicating significant variability. Conversely, the "siElf3" replicates were positioned closely within the PCA plot, reflecting a higher degree of similarity in their gene expression profiles (Figure 8).

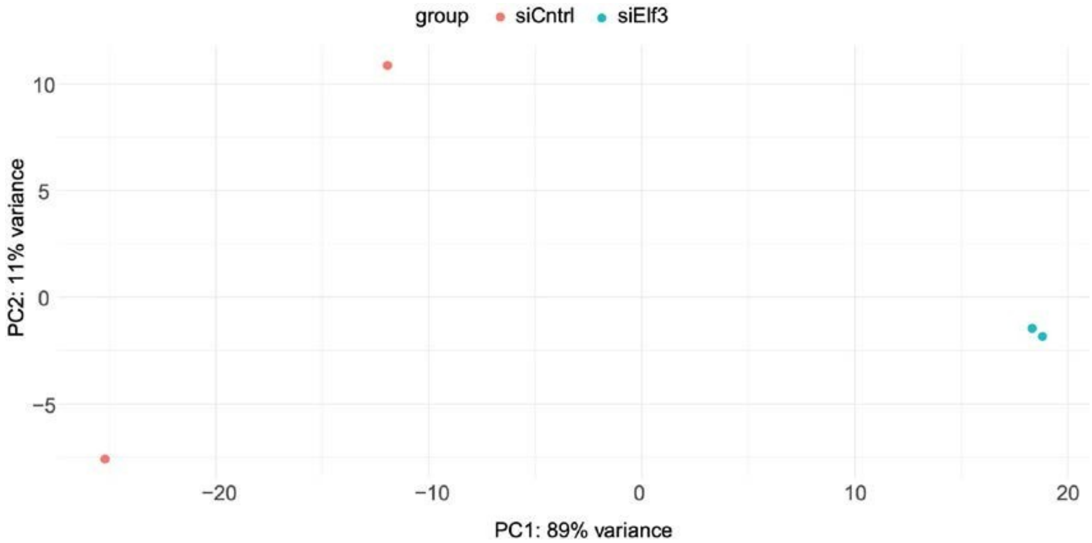

Figure 8. Principal Component Analysis. Two biological replicates, which correspond to the samples from NMuMG cells that were treated with TGFβ3 for 72 hours, were used to generate the PCA plot of the gene expression data obtained using RNA-seq. TGFβ3 treated cells were then washed with PBS for 3 times and transfected with scrambled siRNA (red dots) and from those knocked down of Elf3 (blue dots).

4.2.2. Differential Expression Analysis in Response to Elf3 Silencing During MET

Differential expression analysis between the "siCntrl" and "siElf3" samples yielded a total of 2328 Differentially Expressed Genes (DEGs). These genes were identified based on their p-values being below 0.05 and their absolute log fold change values exceeding 1. The DEG list encompassed 1167 upregulated genes and 1161 downregulated genes. Visual representation was provided through a Volcano plot (Figure 9). This plot effectively illustrates the distribution of differentially expressed genes in terms of their log2 fold change and -log10FDR values. The red dots on the plot signify DEGs that meet the significance criteria in terms of fold change and p-value. In the plot, upregulated genes are positioned on the right side, while downregulated genes occupy the left side. Notably, Elf3 emerges as the most downregulated gene on the volcano plot.

Conversely, the most prominently upregulated gene is Acta2, which is an established mesenchymal marker. Moreover, genes such as Uhrf1, Elf5, H2afx, and Grhl1 are upregulated DEGs, while Itga5 and Gm12925 are downregulated. Furthermore, it is evident from the volcano plot that Cdh1 and Zeb1 fall within the group that exhibits no significant change. The differentially expressed genes were subcategorized based on their properties as proteincoding or long lncRNAs. Table 12 showcases that out of the 1167 upregulated genes, 814 are protein-coding genes, and 209 are lncRNAs.

Similarly, within the 1161 downregulated genes, 918 are protein-coding, while 83 are lncRNAs.

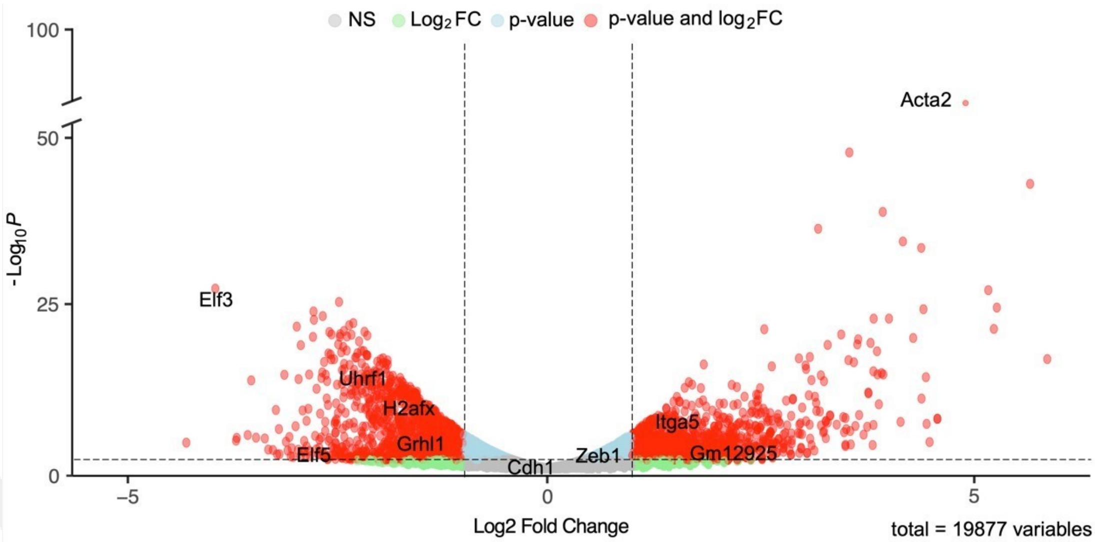

Figure 9. Volcano plot. Volcano plot representation of differential expression analysis of genes in the siCntrl versus siElf3 comparison in NMuMG cell for RNA-seq. The volcano plot shows differentially expressed genes with log2FC >2, p-value > 0.05. Genes significant for both p-value and log2FC values are shown in red, while only pvalues significant genes are shown in blue, only log2FC significant genes in green, and non-significant genes in greys. The x-axis shows log2fold changes in expression, and the y-axis shows the log odds of a gene being differentially expressed. The horizontal dashed line separates genes having log2FC that equals ± 1, and the vertical dashed line separates genes with FDR equal to 0.05.

Table 12. Number of differentially expressed protein-coding and long noncoding RNAs in response to Elf3 silencing.

Upregulated Genes		Downregulated Genes	
1167		1161	
Protein Coding	lncRNA	Protein Coding	lncRNA
814	209	918	83

4.2.3 Gene Ontology Analysis

In pursuit of highlighting the genes marked by collective upregulation and downregulation, a gene ontology analysis was conducted utilizing the RNA-seq data. The results are enlightening: genes experiencing upregulation upon Elf3 silencing are prominently implicated in critical biological processes. Noteworthy among these processes are the negative regulation of cell death and the organization of extracellular cellular and matrix organization. These patterns are succinctly portrayed in Figure 10A. Conversely, genes displaying downregulation upon Elf3 silencing reveal an association with distinct and equally pivotal biological processes. Prominently, these processes encompass DNA replication, nuclear division, chromosome segregation, and a spectrum of cell cycle-related activities. A visual representation of these associations is presented in Figure 10B.

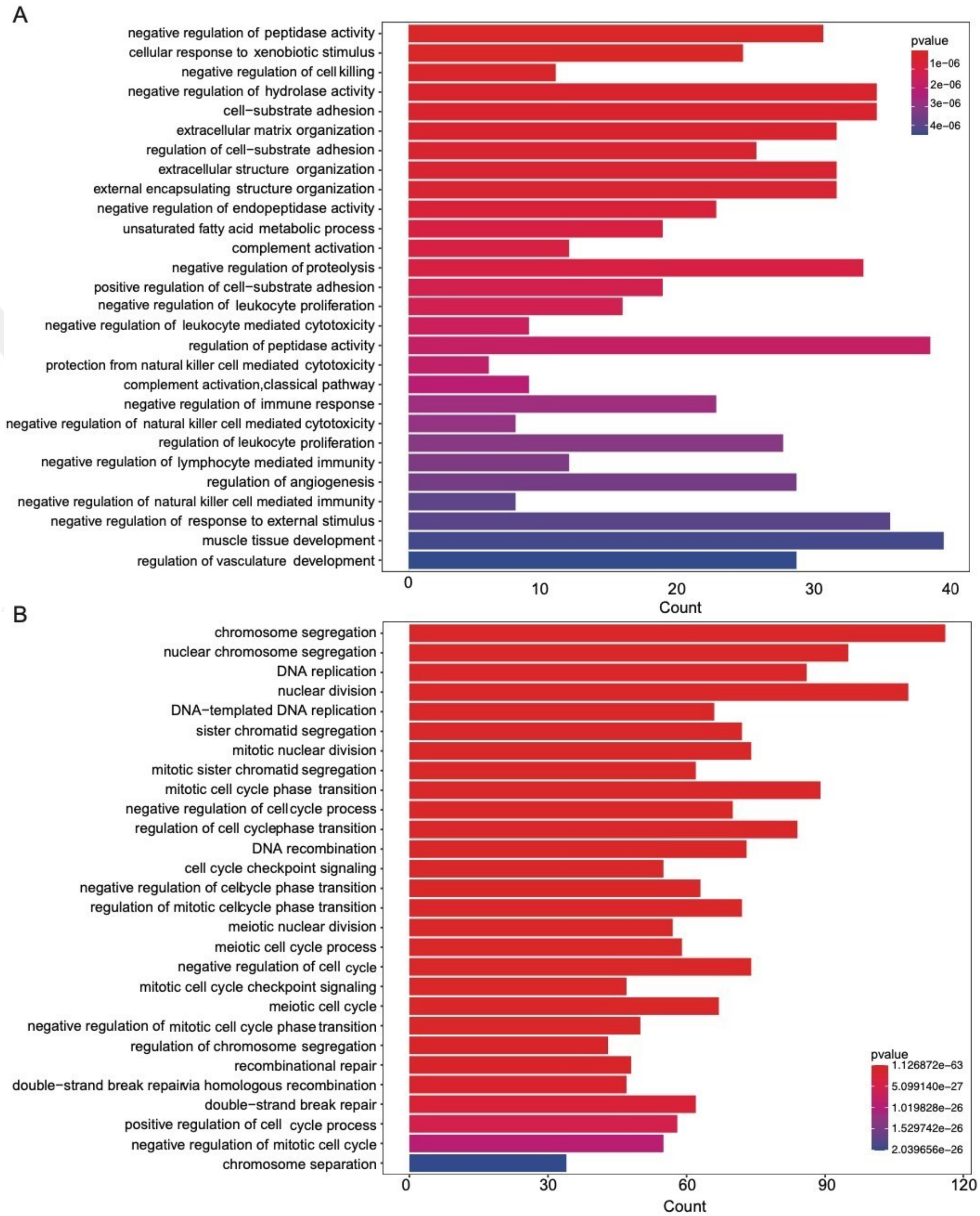

Figure 10. Barplot shows top 25 significant GO terms enriched for Biological Process in response to Elf3 silencing. Biological processes enrichment for upregulated genes (A) and for downregulated genes (B). The X-axis refers to the

number of input genes enriched in the biological process. The color bar shows the pvalue. The red color shows a low p-value, and the blue color shows a high p-value.

4.2.4. Gene Set Enrichment Analysis

Through a systematic application of Gene Set Enrichment Analysis (GSEA), the MSIGDB (The Molecular Signatures Database) Hallmarks were instrumental in shedding light on the intricate landscape of gene enrichment.

The ensuing comparison between siCntrl and siElf3 conditions facilitated the identification of paramount enriched gene sets. The resulting depiction in the Figure is a comprehensive representation of these enriched sets after Elf3 silencing (Figure 11). Investigating the study further reveals fascinating insights, notably the emergence of a select group of highly enriched pathways. Among these, the significance of pathways such as myogenesis, epithelialmesenchymal transition, E2F targets, and DNA repair is particularly pronounced. These insights gleaned from the GSEA analysis substantially enrich our comprehension of the intricate molecular dynamics triggered by Elf3

knockdown.

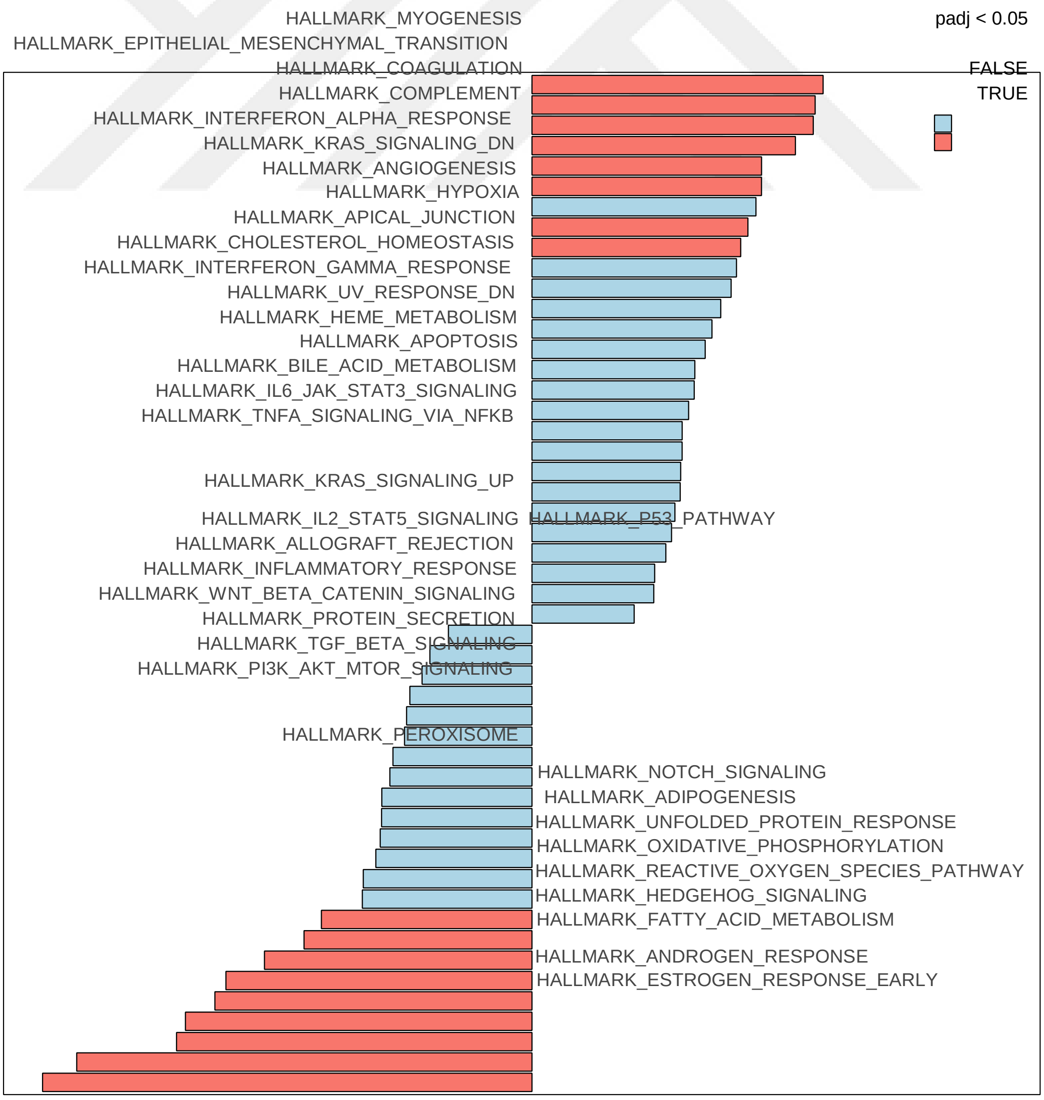

HALLMARK_PANCREAS_BETA_CELLS
HALLMARK_APICAL_SURFACE
HALLMARK_XENOBIOTIC_METABOLISM
HALLMARK_UV_RESPONSE_UP
HALLMARK_GLYCOLYSIS
HALLMARK_ESTROGEN_RESPONSE_LATE

HALLMARK_MTORC1_SIGNALING
HALLMARK_SPERMATOGENESIS
HALLMARK_MITOTIC_SPINDLE HALLMARK_DNA_REPAIR
HALLMARK_MYC_TARGETS_V2
HALLMARK_MYC_TARGETS_V1
HALLMARK_G2M_CHECKPOINT
HALLMARK_E2F_TARGETS
−3 −2 −1 0 1 2 Normalized
Enrichment Score

Figure 11. Gene Set Enrichment Analysis. ene set enrichment analysis of the expression changes (siCntrl versus siElf3) using MSigDB Hallmark gene sets produced a bar plot for the normalized enrichment scores. The red color indicates padj < 0.05.

A heatmap was generated to demonstrate the tangible repercussions of Elf3 knockdown on a specific cluster of genes (Figure 12). This heatmap is a visual beacon, illustrating the subtle changes in gene expression levels within the chosen gene group due to the Elf3 silencing. Remarkably, this heatmap gives a clear explanation: Following Elf3 knockdown, the expression of Snai1, Cebpa, Cdh1, Dnmt1, Uhrf1, and Dnmt3b is dramatically reduced. In contrast, there is a detectable increase in the expression of Cdh2, Dnmt3a, Fn1, Zeb1, Zeb2, Snai2, Hnf4α, and Vimentin.

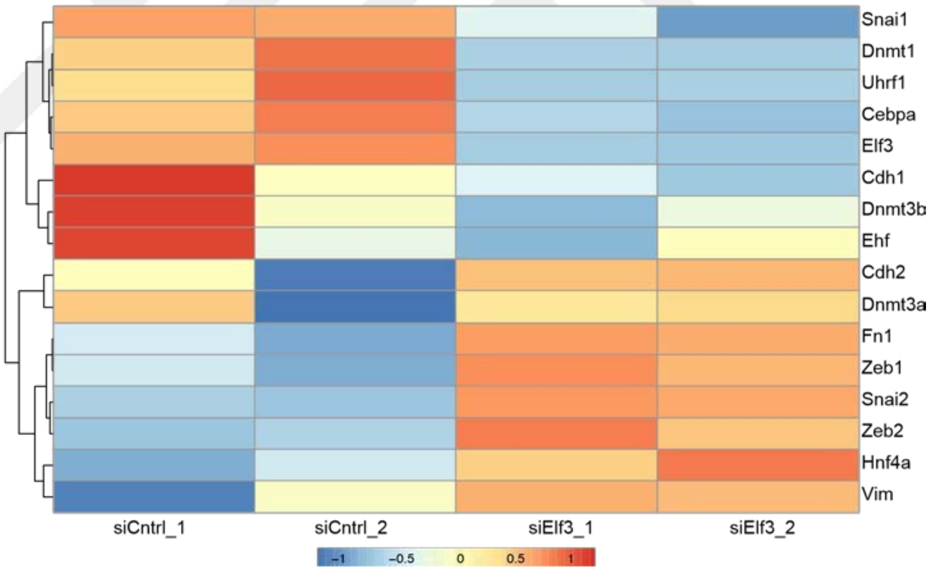

Figure 12. Heatmap representing the expression variances of interested genes. Figure plotted according to log2(RPKM+1) values. Red color represents high expression compared to other samples, while blue represents low expression.

4.3. Elf3 as a Regulator of DNA Methyltransferases

The results obtained from the RNA-seq analysis revealed the downregulation of members of the DNA methylation program in response to Elf3 silencing. This could be attributed to a direct transcriptional regulation by Elf3. To test this hypothesis, we studied the promoters of the DNA methyltransferases for the possibility of Elf3 mediated regulation.

4.3.1. Conservation Analysis and Construction of Reporter Vectors

We reasoned that conserved biological functions would suggest conserved expression patterns, which could imply conserved regulation. Transcriptional regulation requires two main components, a transactivating factor and a cis-regulatory sequence. Considering conserved regulation, one could then assume the conservation of the cis-regulatory sequence(Alotaibi et al., 2010). For this reason, we studied the conservation of the Elf3 binding sites within the promoter regions of the DNA methylatransferases. The transcription factor binding sites of Elf3 were primarily defined via the JASPAR tool to address the potential transcriptional regulatory relationships (Figure 13).

Figure 13. The Elf3 binding site profile as presented by the JASPAR database.

A thorough analysis of the Dnmt1 promoter region positioned roughly 1.5 kb upstream of its Transcription Start Site (TSS) was conducted with precision. This comprehensive investigation encompassed the assessment of conserved sequences and the discernment of potential Elf3 binding sites. Notably, the conservation potential of the Dnmt1 promoter was gauged through the utilization of the ConTra v3 tool, coupled with a cross-species alignment. Remarkably, the 1.5 kb expanse of the Dnmt1 promoter harbors a 14 binding sites for Elf3. Intriguingly, four of these binding sites were situated within sequences of marked conservation (Figure 14. A). Among these, a specific Elf3 binding site exhibited conservation across a spectrum of species, underscoring its functional significance (Figure 14. B). To delve deeper into the practical implications, the 1.5 kb sequence was adeptly cloned into the pGL4.10 vector. This strategic maneuver enabled the quantification of reporter activity in response to Elf3 induction. Subsequently, a pragmatic approach was taken to confirm the minimal essentiality of the promoter, achieved through the careful truncation of the sequence to a length of 1 kb (Figure 14. C).

Similar to Dnmt1, we also analyzed the Uhrf1 promoter region, positioned roughly 1 kb upstream of its TSS. This comprehensive assessment entailed a thorough exploration of conserved sequences alongside the identification of plausible Elf3 binding sites. Of notable significance, the Uhrf1 promoter's degree of conservation was rigorously evaluated utilizing the ConTra v3 tool, closely followed by a meticulous alignment spanning multiple species. Within the span of the 1 kb Uhrf1 promoter, 15 binding sites for Elf3 were astutely delineated. Fascinatingly, five of these binding sites were distinctly situated within sequences characterized by conspicuous conservation (Figure 15. A). Notably, the biologically relevant stature of the two binding sites was accentuated by their conservation across diverse species (Figure 15. B). To glean functional insights, the 1 kb sequence was adroitly inserted into the pGL4.10 vector. This facilitated the quantification of reporter activity in direct response to Elf3 induction. Subsequently, the sequence was meticulously truncated to 750 bp, a deliberate measure to ensure the promoter's true minimalistic essence (Figure 15. C).

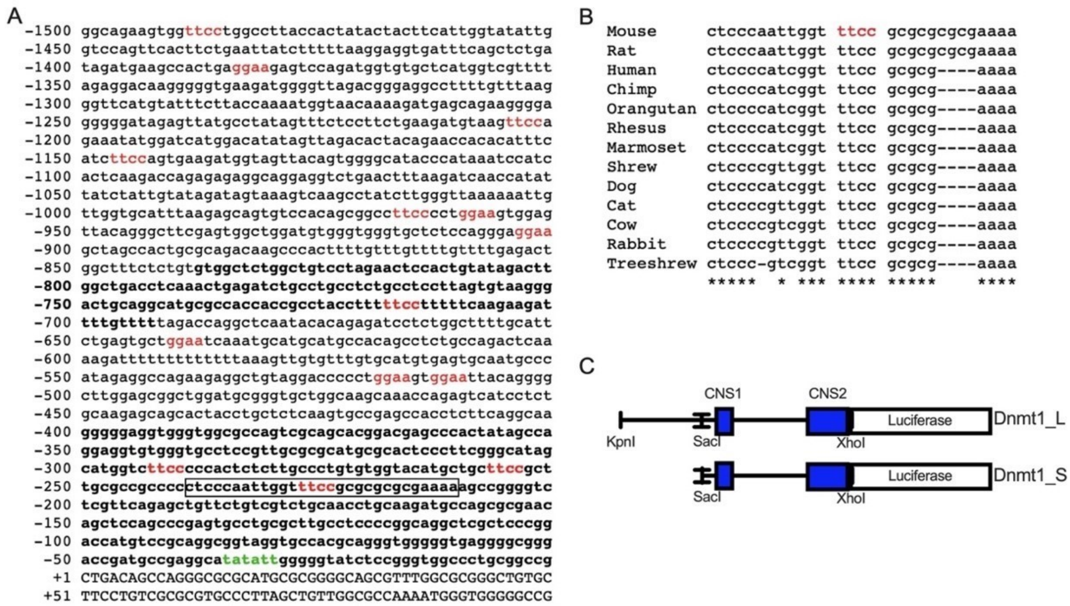

Figure 14. Conserved Elf3 binding sites in the Dnmt1 promoter. Promoter sequence of the Dnmt1 gene, the red sequence shows Elf3 binding sites, the green sequence for the TATA box, and the bold sequences show the conserved sequences. Conservation analysis performed for boxed sequence (A). Sequence alignment of a putative Elf3 binding site in the Dnmt1 promoter showing conservation among different species (B). The cloned promoter schematic representation with the restriction enzymes used to generate the reporter deletions of the promoter is labeled (C).

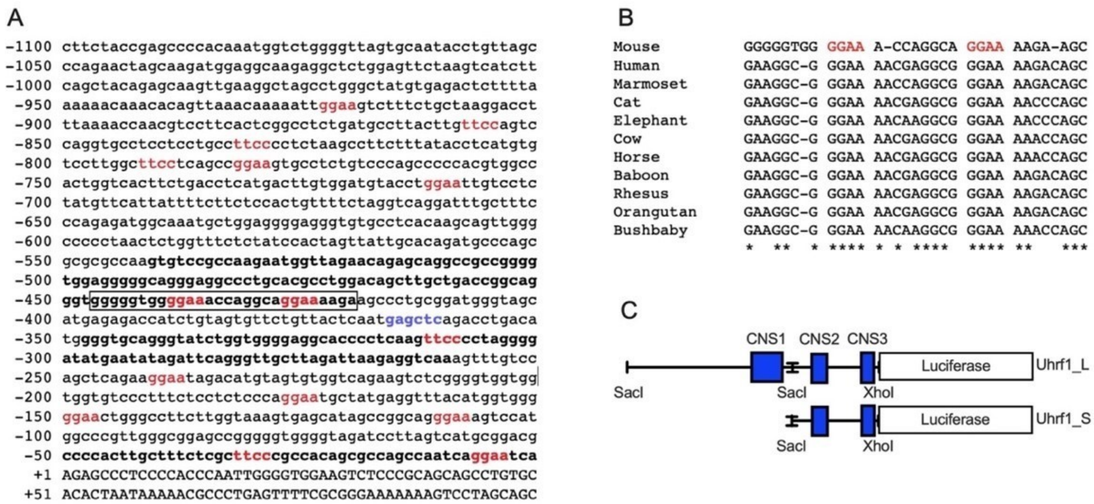

Figure 15. Conserved Elf3 binding sites in the Uhrf1 promoter. Promoter sequence of the Uhrf1 gene, the red sequence shows Elf3 binding sites, and the bold sequences show the conserved sequences. Conservation analysis performed for boxed sequence (A). Sequence alignment of a putative Elf3 binding site in the Uhrf1 promoter showing conservation among different species (B). Cloned promoter schematic representation with the restriction enzymes used to generate the reporter deletions of the promoter is labeled. (C).

We applied the same approach to analyze the promoter region governing Dnmt3b, strategically positioned approximately 1 kb upstream of its TSS. This thorough analysis encompassed a dual perspective: evaluating conserved sequences and identifying plausible Elf3 binding sites. Within the 1 kb span of the Dnmt3b promoter, 14 binding sites for Elf3 were astutely delineated. Significantly, four of these binding sites were distinctively situated within sequences characterized by pronounced conservation (Figure 16. A). Intriguingly, the biological relevance of the three binding sites was strikingly emphasized by their conservation across a spectrum of species (Figure 16. B) The 1 kb sequence was artfully integrated into the pGL4.10 vector to glean functional insights. This 1 kb sequence was cloned in the pGL4.10 vector to measure the reporter activity in response to Elf3 induction (Figure 16. C).

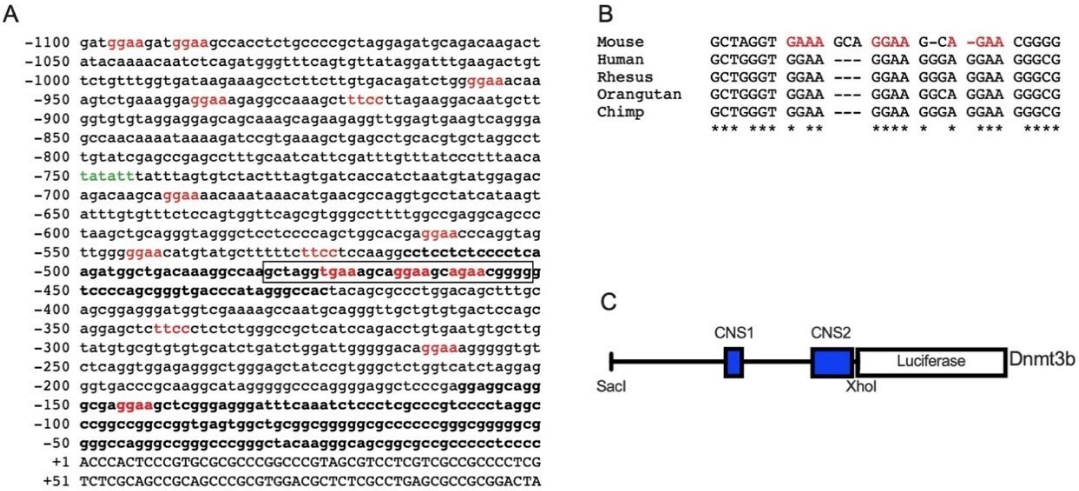

Figure 16. Conserved Elf3 binding sites in the Dnmt3b promoter. Promoter sequence of the Dnmt3b gene, the red sequence shows Elf3 binding sites, and the bold sequences show the conserved sequences. Conservation analysis performed for boxed sequence (A). Sequence alignment of a putative Elf3 binding site in the Dnmt3b promoter showing conservation among different species (B). Cloned promoter schematic representation with the restriction enzymes used to generate the reporter deletions of the promoter are labeled (C).

4.3.2. Luciferase Reporter Activity Measurement

To measure the effect of Elf3 induction on the activity of the cloned promoters, we utilized luciferase reporter assays using NMuMG cells. We observed that the second colony of the *Dnmt1* promoter showed similar promoter activity but with better Elf3 interaction. Additionally, the *Dnmt1* promoter could not retain its promoter activity without the sequence before CNS1 (Figure 17. A-B). However, the interaction with Elf3 was retained. In three colonies of *Uhrf1* promoter, the third colony showed the most convincing promoter activity (Figure 17. C). In the absence of CNS1, the *Uhrf1* promoter could not retain its promoter activity and lost its Elf3 interacting site (Figure 17. D). According to the luciferase reporter assay, 2 colonies of Dnmt3B showed too much difference in interaction with Elf3 but not the promoter activity.

A series of transfection experiments conducted within NMuMG cells explored various lengths of promoter sequences, including multiple colonies from the cloning process. A notable result of this intriguing project emerged: the second colony under the Dnmt1 promoter domain displayed a similar degree of promoter activity and a strengthened propensity for interaction with Elf3. Moreover, the promoter activity of the Dnmt1 promoter proved to be contingent on the presence of the sequence preceding CNS1. Remarkably, despite the absence of this sequence, the interaction with Elf3 remained resilient. Shifting the spotlight to the Uhrf1 promoter, a captivating trend was unveiled: among the three colonies subjected to assessment, the third colony remarkably showcased the most robust promoter activity.

Interestingly, in instances where CNS1 was absent, the Uhrf1 promoter grappled with the retention of its promoter activity. Significantly, this event was accompanied by a discernible loss of Elf3 interacting sites, a phenomenon meticulously confirmed through luciferase assays. A distinctive revelation emerged from the luciferase reporter assay conducted on the Dnmt3B promoter: while the promoter activity remained relatively uniform, two colonies exhibited a pronounced variance in their interaction with Elf3.

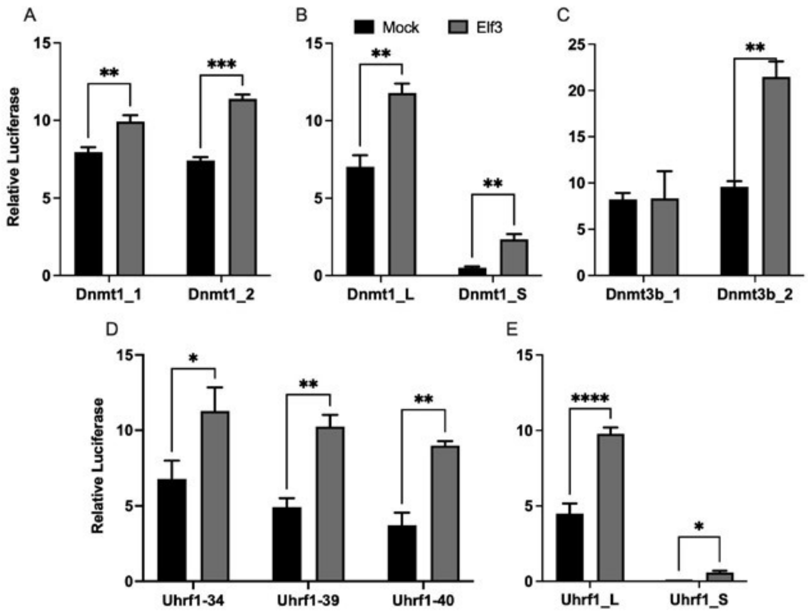

Figure 17. Luciferase reporter assay showing Elf3-mediated promoter activation. Relative luciferase activity is calculated as fold induction relative to the vector. Successfully cloned Dnmt1 promoter activity of 2 different colonies (A), long and short version of Dnmt1 promoter activation by Elf3 (B). Successfully cloned Dnmt3b promoter activity of 2 different colonies (C). Successfully cloned Uhrf1 promoter activity of 2 different colonies (D), long and short version of Uhrf1 promoter activation by Elf3 (E).

4.3.3. Chromatin Immunoprecipitation (ChIP)

To provide evidence for the direct interaction of Elf3 with Dnmt1, Dnmt3b, and Uhrf1 promoters, ChIP assay was performed. The S220 focusedultrasonicator (Covaris, Woburn, MA, USA) was used for a precisely timed span of 30 minutes. Sonication was structured with alternating cycles of 60 seconds on and 60 seconds off, alongside specific parameters including a Peak Power of 140 W, Duty factor of 15, Cycles/burst of 200, and water temperature maintained at 4°C. Subsequent evaluation of the sonicated DNA fragments, undertaken through agarose gel electrophoresis, revealed the distinct bands of fragmented DNA residing within the size range of 500 to 250 base pairs (Figure 18). The binding of Elf3 at the Dnmt1, Dnmt3b, and Uhrf1 promoters was confined during MET by ChIP analysis (Figure 19). ChIP qPCR results was confirmed the reporter assay results. All of the promoters showed statistically significant enrichment in Elf3 ChIP.

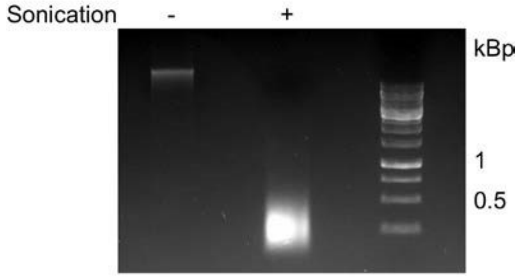

Figure 18. Agarose gel electrophoresis gel image for ChIP. NMuMG cells were treated with TGFβ3 for 72 h; TGFβ3 treated cells were then washed with PBS 3 times and continued incubation for an additional 48 h to initiate MET (post-treatment: PT48). Cells were cross-linked, and a part of DNA was isolated from sonicated DNA to check the quality of sonication.

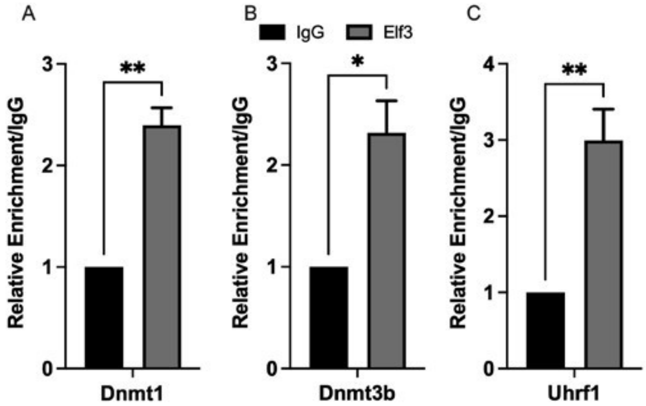

Figure 19. Elf3 binding at the promoters of Dnmt1, Dnmt3b, and Uhrf1. NMuMG cells were treated with TGFβ3 for 72 h; TGFβ3 treated cells were then washed with PBS 3 times and continued incubation for an additional 48 h to initiate MET (posttreatment: PT48). Cells were cross-linked, and chromatin immunoprecipitation was performed. ChIP DNA was used in qPCR to measure the occupancy of Elf3 compared to control antibodies in Dnmt1, Dnmt3b, and Uhrf1 promoters.

4.4. Methylated DNA Immunoprecipitation-hydroxymethylated DNA Immunoprecipitation (MeDIP-hMeDIP)

Genomic DNA was isolated from the successfully undergone EMT-MET cells to examine the methylation status within the promoter regions of epithelial and mesenchymal genes during the EMT-MET transition. Two µg of genomic DNA were used for each immunoprecipitation reaction. The DNA underwent a controlled sonication process in Bioruptor for 20 cycles. The outcomes of this process were subject to validation: unsonicated and sonicated DNAs were thoughtfully loaded onto an agarose gel, ensuring the confirmation of successful sonication. Encouragingly, the gel analysis unveiled a fragmentary pattern within the 200 to 1000 base pairs range, effectively affirming the successful fragmentation achieved through sonication (Figure 20). Following this validation step, the fragmented gDNA was subjected to an Immunoprecipitation (IP) procedure. This meticulous approach serves as a conduit to target specific DNA sequences, in this case, the promoter regions of interest.

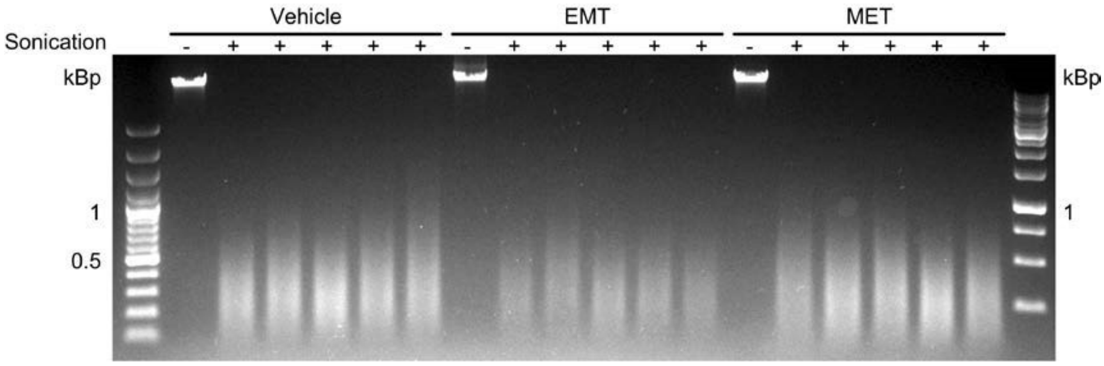

Figure 20. Agarose gel electrophoresis gel image for DIP. Genomic DNA from NMuMG cells was isolated, sonicated, and then checked for correct fragmentation range by agarose electrophoresis.

Following the execution of the meDIP and hMeDIP experiments, the enriched DNA materials underwent an evaluation to detect methylation dynamics residing within the promoter regions of both epithelial and mesenchymal genes. Since DNA methylation at the promoter would infer silencing of gene expression and thus reduced mRNA levels, concordant methylation at the promoter would be expected. Despite the decreased expression of some epithelial genes during EMT (Figure 4), the promoter methylation did not increase. This was evident for Cdh1, Grhl3, Ovol2, and Cebpα (Figure 21. A-D). Cdh1 and Cebpα promoters showed a significant decrease in methylation (Figure 21. A, B), while Ovol2 and Grhl3 promoters showed little decrease (Figure 21. C, B).

On the other hand, Hnf4α and Elf3 promoter methylation was significantly increased (Figure 21. E, F). As expected, the decrease of Hnf4α gene expression was in agreement with the increased methylation of its promoter during EMT. Another observation takes center stage: Despite a prolonged 3-day TGFβ3 treatment, the relative expression of Elf3 exhibited resilience. However, this resilient expression contrasted sharply with the scenario unfolding on its promoter region, which underwent a marked increase in methylation during EMT. During MET, epithelial genes show an increased expression. Therefore, a decrease is expected in the methylation of these genes.

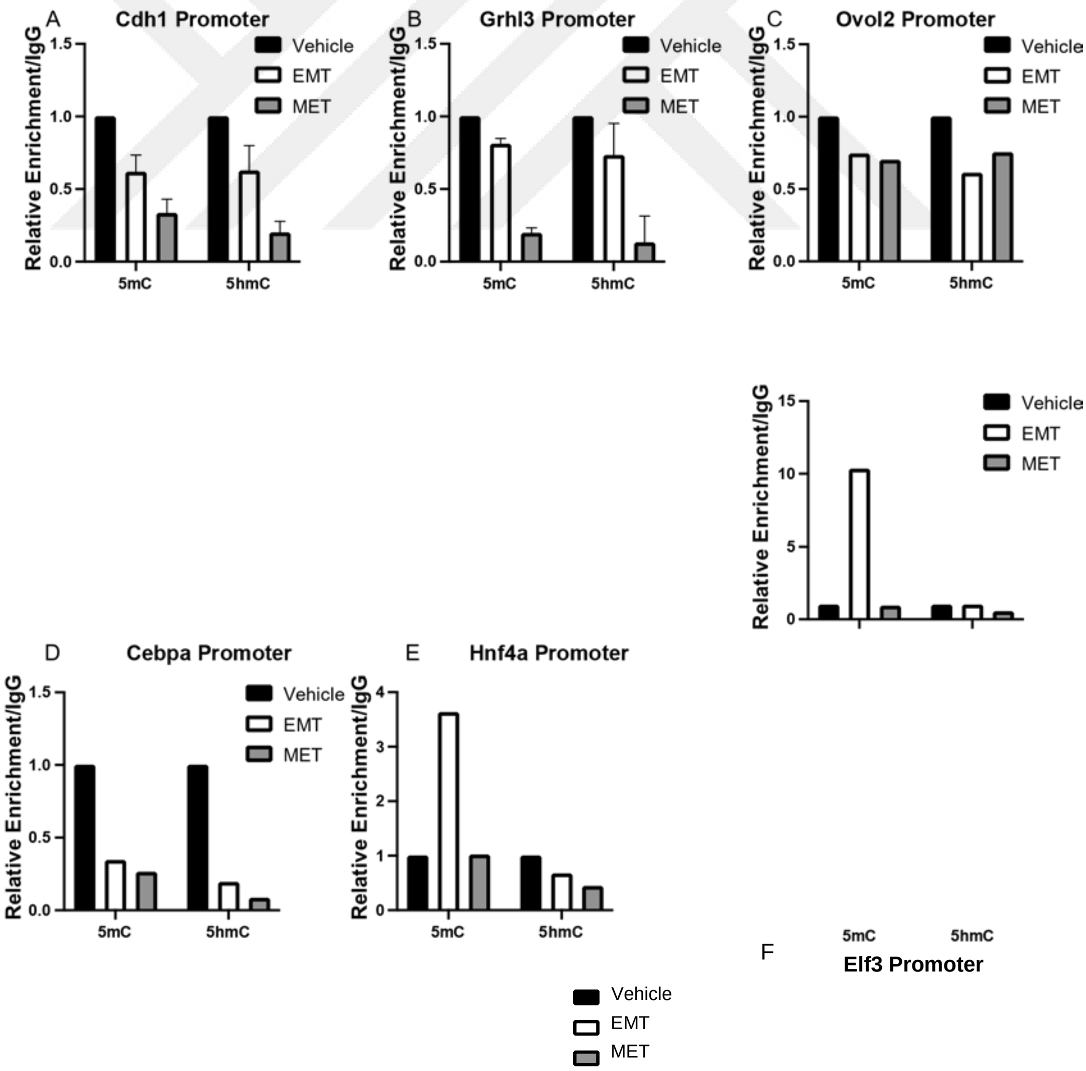

Figure 21. Methylation states of epithelial genes during EMT-MET. meDIP and hMeDIP, DNA of EMT/MET, was used in qPCR to measure the occupancy of epithelial genes. The relative expression levels of Cdh1 (A), Grhl3 (B), Ovol2 (C), Cebpa (D), Hnf4a (E) promoters in meDIP and hMeDIP during EMT-MET in NMuMG cells.

In the context of mesenchymal genes, the observed promoter methylation patterns aligned with the expected outcomes of their expression levels (Figure 5.)**.** Notably, genes that exhibited increased gene expression demonstrated a corresponding decrease in promoter methylation. This was evident in the cases of Zeb1 and Zeb2 (Figure 22. A, B). Interestingly, despite the noted increase in gene expression for Snai1 (Figure 22. C), methylation of its promoter region was not changed during the EMT phase. During the MET phase, a distinctive trend emerged: while the relative gene expressions of mesenchymal genes underwent a reduction, the corresponding promoter methylation levels did not surpass those observed during the EMT phase. This observation underscores the intricate dynamics governing gene expression and promoter methylation during these transition phases.

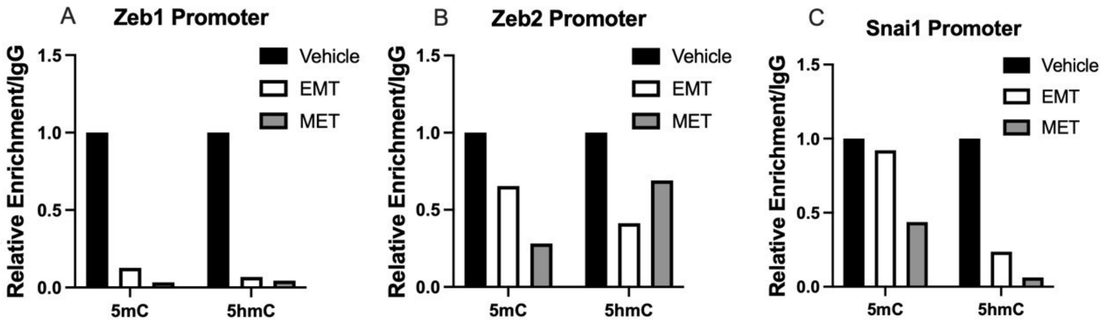

Figure 22. The methylation states of mesenchymal genes during EMT-MET. meDIP and hmeDIP, DNA of EMT/MET, was used in qPCR to measure the occupancy of mesenchymal genes. The relative expression levels of Zeb1(A), Zeb2(B), and Snai1(C) promoters in meDIP and hmeDIP during EMT/MET in NMuMG cells.

Following the strategic siElf3 intervention, a comprehensive array of meDIP and hmeDIP experiments was performed. DNA was isolated from successfully silenced Elf3 cells, and two µg of genomic DNA was subjected to sonication for each sample, resulting in DNA fragmentation within the 2001000 bp range. The fragmentated DNA was used for DIP.

The 5mC or 5hmC enriched DNAs, were subsequently subjected to a comprehensive evaluation aimed at deciphering the methylation dynamics within the promoter regions of both epithelial and mesenchymal genes.

According to our previous knowledge base, the outcomes of the qPCR assays and the insights gleaned from the confocal images collectively reaffirmed the influence of Elf3 knockdown on the MET process. This knowledge was further fortified through the meticulous analysis of siElf3 RNAseq data. Intriguingly, Elf3 silencing emerged as a pivotal determinant impacting the expressions of genes distinctively linked to epithelial and mesenchymal states. For instance, Cdh1 and Cebpa (Figure 23. A, D) expressions showed a noticeable reduction following Elf3 silencing. Notably, a corresponding surge in promoter methylation levels was prominently evident. This intricate relationship was further highlighted by observing increased promoter methylation in genes like Ovol2, Grhl3, and Hnf4a (Figure 23. C, B, and E). Turning the focus to mesenchymal genes, a distinct trend emerged: except for Snai1 (Figure 24. C), the silencing of Elf3 exerted an adverse influence on Zeb1, Zeb2, and Snai1 (Figure 24. A, B, and C). Notably, a compelling contrast was observed in the context of promoter methylation, as levels for Zeb1, Zeb2, and Snai1 notably decreased. An intriguing correlation surfaced between promoter hydroxymethylation and methylation status, further underscoring the intricate interplay between these regulatory elements.

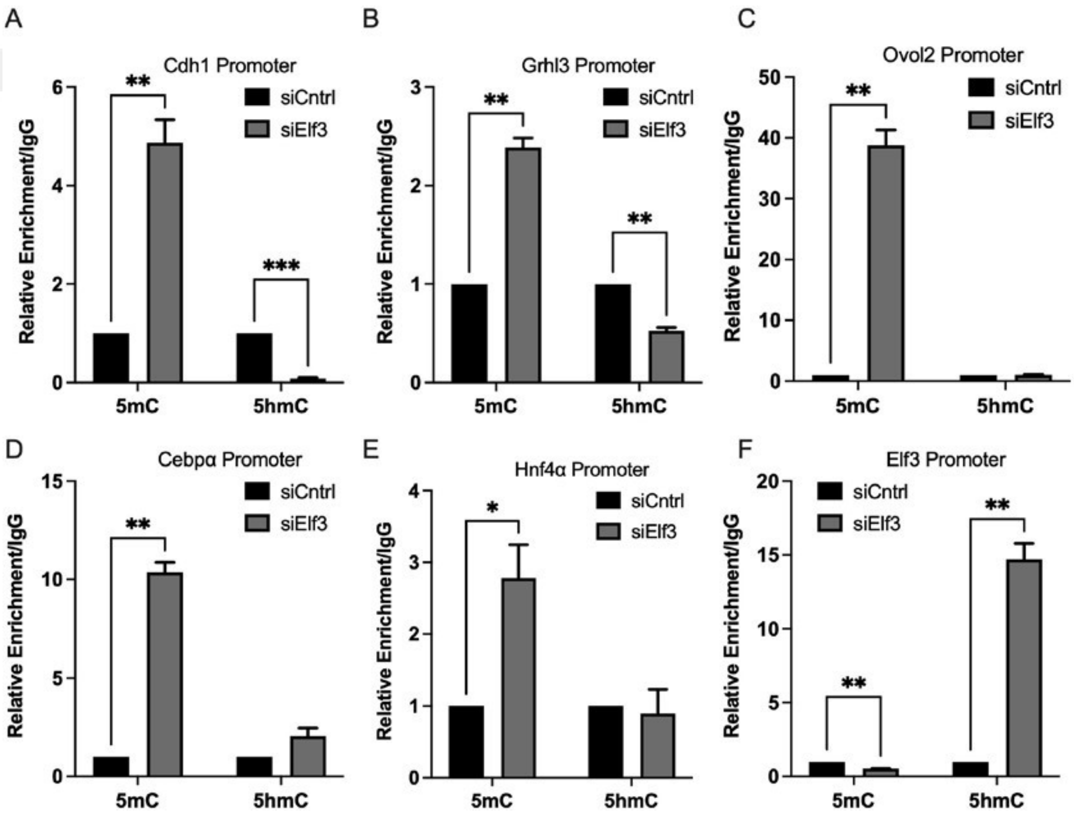

Figure 23. Promoter methylation of epithelial genes in response to Elf3 silencing during MET. meDIP and hmeDIP DNA of siElf3 were used in qPCR to measure the occupancy of epithelial genes. The relative expression levels of Cdh1 (A), Grhl3 (B), Ovol2 (C), Cebpα (D), Hnf4α (E) promoters in me-DIP and hme-DIP during siElf3 in MET in NMuMG in NMuMG cells.

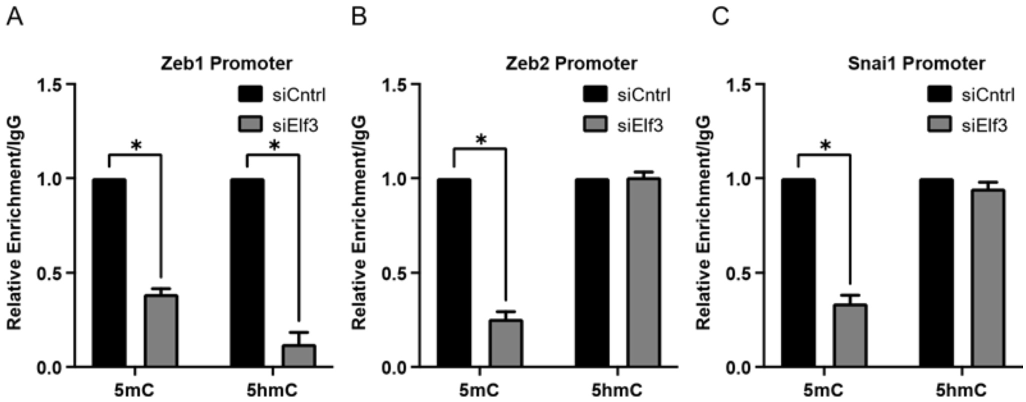

Figure 24. Promoter methylation of mesenchymal genes genes in response to Elf3 silencing during MET. meDIP and hMeDIP DNA of siElf3 was used in qPCR to measure the occupancy of mesenchymal genes. The relative expression levels of Zeb1(A), Zeb2(B), Snai1(C) promoters in meDIP and hMeDIP during siElf3 in MET in NMuMG cells.

5. DISCUSSION

Several epigenetic mechanisms are crucial for determining cellular identity, including DNA methylation, lncRNAs, repetitive DNA elements, and histone variants (Bogdanović and Lister, 2017; Hardman, 1986; Salviano-Silva et al., 2018). These epigenetic mechanisms determine the gene expression status; therefore, they are crucial for several biological processes in health and disease.

Previous laboratory studies identified transcription factors specific to the epithelial state based on their correlation with Cdh1 expression. The transition between EMT and MET involves a shift in the expression of cadherin genes. E-cadherin, an adhesion molecule, plays a crucial role in maintaining the epithelial state, and its control is precisely managed during various developmental and physiological processes. The effective execution of MET depends on the positive regulation of Cdh1 expression. This implies that factors governing Cdh1 expression also govern MET and the epithelial state. Elf3, Grhl3, and Ovol2 were among the transcription factors identified, and they showed a significant association with the epithelial phenotype.

Additionally, Elf3 appeared to be essential for proper MET progression. Depletion of Elf3 caused a severe MET defect marked by the absence of Ecad from the plasma membrane and the downregulation of several epithelial genes, particularly Grhl3. Elf3 was identified as a regulator of Grhl3 expression after closely examining the connection between Elf3 and Grhl3 (Sengez et al., 2019). In cells undergoing MET, Elf3 was enriched at the promoter of Grhl3. Our preliminary data suggested that Elf3 and Grhl3 might regulate the PCNA/DNMT1/UHRF1 complex, which is necessary for maintaining global DNA methylation.

Epigenetic changes are crucial for many biological processes, which are reversible, independent of DNA sequence, and can influence gene activity and expression. DNA methylation is one of the best-characterized epigenetic modifications primarily catalyzed by DNA methyltransferases (DNMTs) (Jin et al., 2011; Rajabi et al., 2016; Varriale, 2014) and is essential for development, genome defense, genome imprinting, and X-chromosome inactivation, and misregulation of DNA methylation has been implicated in disease (Bird, 2007) . There are three DNMTs in mammals: DNMT1, DNMT3A, and DNMT3B (Liao et al., 2015; Tajima et al., 2016). This biochemical process regulates gene expression and is commonly associated with transcriptional repression (Curradi et al., 2002). It has been shown that DNMTs are upregulated in cancers (Jin and Robertson, 2013; Subramaniam et al., 2014). DNMT1 maintains methylation during DN replication (Robert et al., 2003; Tajima et al., 2016). However, DNMT3a and DNMT3b are de novo DNA methyltransferases responsible for catalyzing the methylation of cytosines (Oka et al., 2005). UHRF1 (Ubiquitin-like containing PHD and Ring Finger domain 1) is an epigenetic factor responsible for maintaining DNA CpG methylation, chromatin remodeling, and regulation of gene expression (Liu et al., 2013). Many studies demonstrated that it is upregulated in several cancer models, such as lung, liver, and breast cancers (Gao et al., 2017; Kofunato et al., 2012). Lack of UHRF1 is correlated with an increased migratory capacity of cells through EMT (Kim et al., 2017). It is also shown that the downregulation of UHRF1 enhances the migratory and invasive properties of human cancer cells by inducing EMT via the CXCR4 signaling pathway. Separation of PCNA/DNMT1/UHRF1 complex is associated with global DNA hypomethylation. DNMT1 binds to proliferating cell nuclear antigen (PCNA) at DNA damage sites (Schermelleh et al., 2007).

Here, we first analyzed RNA-seq data of NMuMG cells in the absence of Elf3 during mesenchymal to epithelial transition to observe transcriptome dynamics. Expression changes of DNA methylation enzymes Dnmt1, Uhrf1, and Dnmt3b were identified. With unrecovered Cdh1 expression during MET in response to Elf3 depletion, Dnmt1 and Uhrf1 expression has significantly decreased. On the other hand, Dnmt3b expression decrease was not significant. Furthermore, the GO enrichment analysis conducted on genes that were downregulated following the silencing of Elf3 highlighted their involvement in specific and equally essential biological processes. Notably, these processes encompass functions such as DNA replication, nuclear division, chromosome segregation, and a range of activities related to the cell cycle. It is known that DNA methylation influences replication time and replication fork progression (Probst et al., 2009).

DNA methylation patterns must be faithfully maintained in daughter strands during replication. The nuclear division includes processes such as mitosis and meiosis, where the cell's nucleus divides to ensure the proper distribution of genetic material. DNA methylation can impact nuclear division in the epigenetic inheritance, chromosome segregation, centromere function, and chromosomal instability (Wu and Zhang, 2014). GSEA notably the emergence of a select group of highly enriched pathways. Particularly notable are the pathways involved in myogenesis, the epithelial-mesenchymal transition, E2F targets, and DNA repair. DNA methylation contributes to myogenesis, the muscle cell formation and differentiation process (Lucarelli et al., 2001). During myogenesis, DNA methylation patterns are dynamically regulated to control the expression of genes involved in muscle development. E2F transcription factors are critical regulators of the cell cycle and are involved in processes such as cell proliferation and apoptosis (Dyson, 1998). DNA methylation can affect E2F target genes by cell cycle regulation and suppression of tumors (Massenet et al., 2021).

DNA methylation is located on the 5'-carbon of the cytosine in cytosinephosphate-guanine (CpG) sequences (Deaton and Bird, 2011; Jeziorska et al., 2017). The methylation of cytosine at CpG sequences is the primary DNA methylation in mammals and is regulated in a tissue-specific manner (L. D. Moore et al., 2013). CpG sequences are likely to cluster in CpG islands (CGIs) (Deaton and Bird, 2011). CpG cytosines are known to be substantially methylated (~3 × 107), a heritable mark of gene silencing (Jang et al., 2017).

DNA methylation can also cluster at cytosine–phosphate–adenine (CpA), cytosine–phosphate–thymine (CpT), and cytosine–phosphate–cytosine (CpC) sequences (Patil et al., 2014). Methylated CpG nucleotides are localized in repetitive DNA elements, including short and long-interspersed nuclear elements (SINEs and LINEs), gene bodies, and centromeres (Papin et al., 2017). However, CGIs usually contain unmethylated sequences (Deaton and Bird, 2011; Yamada et al., 2004). Cytosines (C) are found in two forms: unmethylated and methylated (5mC), which is often referred to as the fifth base of DNA in mammals (Breiling and Lyko, 2015). 5mC is a key state associated with various processes such as gene regulation, development, genomic imprinting, X-chromosome inactivation, and differentiation (Hackett and Azim Surani, 2013; SanMiguel and Bartolomei, 2018). Although researchers have gained a great deal of knowledge about DNA methylation, which acts as a key regulator of cell identity establishment (Bogdanović and Lister, 2017), gaps remain in our knowledge of DNA methylation. Therefore, it is essential to understand its dynamic nature to uncover many of the unknowns about this complex event.

DNA hydroxymethylation is considered an essential intermediate of the demethylation process step and usually indicates a hallmark of transcriptional activation, opposite to the effect of DNA methylation. DNA hydroxymethylation is another DNA modification in which the hydrogen atom at the C5 position is replaced by a hydroxymethyl (Guibert and Weber, 2013; Richa and Sinha, 2014). This recent type of DNA modification gained interest due to its biological and epigenetic roles in cellular systems, including differentiation, development, and pluripotency (Richa and Sinha, 2014). 5- hydroxymethylcytosine (5-hmC) is formed by oxidation of 5mC by the Ten-Eleven Translocation (TET) family of proteins, including TET1, TET2, and TET3 and considered as “6th base” (Münzel et al., 2011; Santiago et al., 2014). It is an intermediate step in active DNA demethylation reaction and essential for chromatin factors. DNA methylation is one of the key events among epigenetic mechanisms; maintenance of repetitive elements also significantly impacts regulatory changes and genome stability.

Most current studies focus on comprehending how alterations in gene expression, driven by epigenetic events, play a role in EMT. This area has gained significant attention recently. The growing body of evidence underscores the significance of epigenetic mechanisms in EMT, particularly in relation to transcription factors (TFs) and histone variants (Monteiro-Reis et al., 2019). While MET holds importance in both normal development and disease contexts (Chaffer et al., 2016), there have been limited endeavors to understand the specific transcription factors influencing the epigenetic landscape of MET.

Although bisulfite sequencing was considered the most accurate method for studying the methylome, recent results show that the bisulfite method cannot differentiate between 5mC and 5hmC (Adusumalli et al., 2014) and thus hinders our understanding of the dynamics associated with gene expression in relation to DNA methylation. MeDIP and hMeDIP have emerged as invaluable tools for investigating the epigenetic changes accompanying EMT and MET. By comparing the methylation patterns of cells undergoing these transitions to those in stable states, differential DNA methylation regions could be defined. Additionally, MeDIP and hMeDIP offer a comprehensive view of the connection between DNA methylation and the binding of transcription factors across the genome. The interaction between these epigenetic indicators and the functioning of transcription factors plays a crucial role in ensuring the accurate timing and implementation of EMT and MET processes.

To elucidate the epigenetic mechanism of regulation of gene expression by Elf3, we first established validated external controls for ChIP-qPCR, MeDIP-qPCR, and hMeDIP-qPCR assays to normalize the variations introduced during the assays. We have determined the methylation and hydroxymethylation levels of epithelial and mesenchymal markers in EMT and MET. We also have determined the methylation and hydroxymethylation levels of epithelial and mesenchymal markers in the absence of Elf3 in MET. In order to normalize the quantification of relative enrichment of the target region in qPCR, which may be followed by next-generation sequencing analysis, it is important to include external control fragments in these assays. This is indicated by the results of the relatively large deviations of positive controls in technical replicates in MeDIP, hMeDIP, and ChIP.

6. CONCLUSION AND SUGGESTIONS

Within the scope of the thesis project, experimental validation of Dnmt1, Uhrf1, and Dnmt3b by in-silico analyses confirmed the critical importance of the promoters and Elf3 interaction investigated by luciferase assay and Elf3ChIP and, according to transcriptome data of siElf3 in MET, expression of related genes decreased compared to siCntrl. In addition to data analysis, the absence of Elf3 affects most of the pathways related to DNA methylation. Experiment results of luciferase assay and Elf3-ChIP concluded that Elf3 and promoters of related genes were highly interactive. In conservation analysis of the promoter regions, we observed that most of the Elf3 binding sites on the promoter were conserved between organisms. Elf3-ChIP also showed high relative expression on the promoters of related genes. This experiments strongly pointed to the relationship of Elf3 with these genes.

Additionally, we investigated the methylation and hydroxymethylation profiles of EMT-MET after the silencing of Elf3 during MET. In a proper EMT, expression levels of epithelial genes decrease, and mesenchymal genes vice versa. A change of a gene expression mirrors methylation levels of promoters similarly. Hnf4α and Elf3, promoter methylation levels, are significantly increased in EMT, and during MET, the methylation was restored to the epithelial state levels. Both of the gene promoter methylation did not show any change. When we examine Grhl3 and Ovol2 in EMT, promoter methylation of this transcription factor has not shown any change. On the other hand, we have observed a decrease in promoter methylation of Grhl3 in MET but no change in Ovol2. Unexpectedly, Cdh1 and Cebpα were shown to decrease in promoter methylation in EMT and, expectedly, also in MET.

As our previous knowledge about the absence of Elf3 causes impaired MET, we observed an increase in promoter methylation in epithelial genes and a decrease in mesenchymal genes, as expected. In future research, other than RNA-seq data, MeDIP-seq and hMeDIP-seq of EMT-MET timepoints and siElf3 MET should be coupled to investigate the place of Elf3 in DNA methylation. Additionally, other NGS technologies, such as ChIP-seq or CUT&RUN-seq, should be performed for Elf3 to investigate its occupancy in order to define its transcriptional targets.

7. REFERENCES

Adhikari, D., Diril, M. K., Busayavalasa, K., Risal, S., Nakagawa, S., Lindkvist, R., … Liu, K. 2014. "Mastl is required for timely activation of APC/C in meiosis I and Cdk1 reactivation in meiosis II". Journal of Cell Biology, *206*(7), 843–853.

Adusumalli, S., Omar, M. F. M., Soong, R., Benoukraf, T. 2014. "Methodological aspects of whole-genome bisulfite sequencing analysis". Briefings in Bioinformatics.

Alotaibi, H., Basilicata, M. F., Shehwana, H., Kosowan, T., Schreck, I., Braeutigam, C., … Stemmler, M. P. 2015. "Enhancer cooperativity as a novel mechanism underlying the transcriptional regulation of E-cadherin during mesenchymal to epithelial transition". Biochimica et Biophysica Acta (BBA) - Gene Regulatory Mechanisms, *1849*(6), 731–742.

Alotaibi, H., Yaman, E., Salvatore, D., di Dato, V., Telkoparan, P., di Lauro, R., Tazebay, U. H. 2010. "Intronic elements in the Na+/I- symporter gene (NIS) interact with retinoic acid receptors and mediate initiation of transcription". Nucleic Acids Research.

Andreoli, J. M., Jang, S.-I., Chung, E., Coticchia, C. M., Steinert, P. M., Markova, N. G. 1997. "The expression of a novel, epithelium-specific ets transcription factor is restricted to the most differentiated layers in the epidermis". Nucleic Acids Research, *25*(21), 4287–4295.

Bakir, B., Chiarella, A. M., Pitarresi, J. R., Rustgi, A. K. 2020. "EMT, MET, Plasticity, and Tumor Metastasis". Trends in Cell Biology, *30*(10), 764–776.

Banyard, J., Bielenberg, D. R. 2015. "The role of EMT and MET in cancer dissemination". Connective Tissue Research.

Bedzhov, I., Alotaibi, H., Basilicata, M. F., Ahlborn, K., Liszewska, E., Brabletz, T., Stemmler, M. P. 2013. "Adhesion, but not a specific cadherin code, is indispensable for ES cell and induced pluripotency". Stem Cell Research, *11*(3), 1250–1263.

Bird, A. 2007. "Perceptions of epigenetics". Nature.

Bogdanović, O., Lister, R. 2017. "DNA methylation and the preservation of cell identity". Current Opinion in Genetics and Development.

Brabletz, S., Bajdak, K., Meidhof, S., Burk, U., Niedermann, G., Firat, E., … Brabletz, T. 2011. "The ZEB1/miR-200 feedback loop controls Notch signalling in cancer cells". The EMBO Journal, *30*(4), 770–782.

Breiling, A., Lyko, F. 2015. "Epigenetic regulatory functions of DNA modifications: 5-methylcytosine and beyond". Epigenetics and Chromatin.

Canel, M., Serrels, A., Frame, M. C., Brunton, V. G. 2013. "E-cadherin–integrin crosstalk in cancer invasion and metastasis". Journal of Cell Science, *126*(2), 393–401.

Cattin, A.-L., Le Beyec, J., Barreau, F., Saint-Just, S., Houllier, A., Gonzalez,

F. J., … Ribeiro, A. 2009. "Hepatocyte Nuclear Factor 4α, a Key Factor for Homeostasis, Cell Architecture, and Barrier Function of the Adult Intestinal Epithelium". Molecular and Cellular Biology, *29*(23), 6294–6308.

Chaffer, C. L., San Juan, B. P., Lim, E., Weinberg, R. A. 2016. "EMT, cell plasticity and metastasis". Cancer and Metastasis Reviews.

Chapnick, D. A., Warner, L., Bernet, J., Rao, T., Liu, X. 2011. "Partners in crime: The TGFβ and MAPK pathways in cancer progression". Cell and Bioscience.

Chen, J., Han, Q., Pei, D. 2012. "EMT and MET as paradigms for cell fate switching". Journal of Molecular Cell Biology, *4*(2), 66–69.

Chen, T., You, Y., Jiang, H., Wang, Z. Z. 2017. "Epithelial-mesenchymal transition (EMT): A biological process in the development, stem cell differentiation, and tumorigenesis". Journal of Cellular Physiology, *232*(12), 3261–3272.

Choi, J., Lee, M., Lee, J., Kang, D., Choi, J.-Y. 2017. "Correlates associated with participation in physical activity among adults: a systematic review of reviews and update". BMC Public Health, *17*(1), 356.

Choi, S. S., Diehl, A. M. 2009. "Epithelial-to-mesenchymal transitions in the liver". Hepatology, *50*(6), 2007–2013.

Cicchini, C., de Nonno, V., Battistelli, C., Cozzolino, A. M., De Santis Puzzonia, M., Ciafrè, S. A., … Tripodi, M. 2015. "Epigenetic control of EMT/MET dynamics: HNF4α impacts DNMT3s through miRs-29". Biochimica et Biophysica Acta (BBA) - Gene Regulatory Mechanisms, *1849*(8), 919–929.

Cooper, C. D. O., Newman, J. A., Gileadi, O. 2014. "Recent advances in the structural molecular biology of Ets transcription factors: interactions, interfaces and inhibition". Biochemical Society Transactions, *42*(1), 130–138.

Curradi, M., Izzo, A., Badaracco, G., Landsberger, N. 2002. "Molecular Mechanisms of Gene Silencing Mediated by DNA Methylation". Molecular and Cellular Biology.

De Jaeghere, E. A., Denys, H. G., De Wever, O. 2019. "Fibroblasts Fuel Immune Escape in the Tumor Microenvironment". Trends in Cancer.

Deaton, A. M., Bird, A. 2011. "CpG islands and the regulation of transcription". Genes and Development.

Diepenbruck, M., Christofori, G. 2016. "Epithelial–mesenchymal transition (EMT) and metastasis: yes, no, maybe?". Current Opinion in Cell Biology, *43*, 7–13.

Domaschenz, R., Kurscheid, S., Nekrasov, M., Han, S., Tremethick, D. J. 2017. "The Histone Variant H2A.Z Is a Master Regulator of the EpithelialMesenchymal Transition". Cell Reports, *21*(4), 943–952.

Dubois, V., Staels, B., Lefebvre, P., Verzi, M., Eeckhoute, J. 2020. "Control of Cell Identity by the Nuclear Receptor HNF4 in Organ Pathophysiology". Cells, *9*(10), 2185.

Duncan, E. J., Gluckman, P. D., Dearden, P. K. 2014. "Epigenetics, plasticity, and evolution: How do we link epigenetic change to phenotype?". Journal of Experimental Zoology Part B: Molecular and Developmental Evolution, *322*(4), 208–220.

Dyson, N. 1998. "The regulation of E2F by pRB-family proteins". Genes and Development.

Erami, Z., Timpson, P., Yao, W., Zaidel-Bar, R., Anderson, K. I. 2015. "There are four dynamically and functionally distinct populations of E-cadherin in cell junctions". Biology Open, *4*(11), 1481–1489.

Fazilaty, H., Rago, L., Kass Youssef, K., Ocaña, O. H., Garcia-Asencio, F., Arcas, A., … Nieto, M. A. 2019. "A gene regulatory network to control EMT programs in development and disease". Nature Communications, *10*(1), 5115.

Frisch, S. M., Farris, J. C., Pifer, P. M. 2017. "Roles of Grainyhead-like transcription factors in cancer". Oncogene.

Gajewski, T. F., Schreiber, H., Fu, Y. X. 2013. "Innate and adaptive immune cells in the tumor microenvironment". Nature Immunology.

Gajulapalli, V. N. R., Samanthapudi, V. S. K., Pulaganti, M., Khumukcham, S. S., Malisetty, V. L., Guruprasad, L., … Manavathi, B. 2016. "A transcriptional repressive role for epithelial-specific ETS factor ELF3 on oestrogen receptor alpha in breast cancer cells". Biochemical Journal, *473*(8), 1047–1061.

Gao, S. P., Sun, H. F., Li, L. D., Fu, W. Y., Jin, W. 2017. "UHRF1 promotes breast cancer progression by suppressing KLF17 expression by hypermethylating its promoter". American Journal of Cancer Research.

Giannelli, G., Koudelkova, P., Dituri, F., Mikulits, W. 2016. "Role of epithelial to mesenchymal transition in hepatocellular carcinoma.". Journal of Hepatology, *65*(4), 798–808.

Gibney, E. R., Nolan, C. M. 2010. "Epigenetics and gene expression". Heredity, *105*(1), 4–13.

Gibson, G. 2008. "The environmental contribution to gene expression profiles". Nature Reviews Genetics.

Guibert, S., Weber, M. 2013. "Functions of DNA Methylation and Hydroxymethylation in Mammalian Development". In *Current Topics in Developmental Biology*.

Guo, F., Parker Kerrigan, B. C., Yang, D., Hu, L., Shmulevich, I., Sood, A. K., … Zhang, W. 2014. "Post-transcriptional regulatory network of epithelialtomesenchymal and mesenchymal-to-epithelial transitions.". Journal of Hematology & Oncology, *7*(2), 19.

Gupta, P. B., Pastushenko, I., Skibinski, A., Blanpain, C., Kuperwasser, C. 2019. "Phenotypic Plasticity: Driver of Cancer Initiation, Progression, and Therapy Resistance.". Cell Stem Cell, *24*(1), 65–78.

Gustavsson, P., Copp, A. J., Greene, N. D. E. 2008. "Grainyhead genes and mammalian neural tube closure". Birth Defects Research Part A: Clinical and Molecular Teratology, *82*(10), 728–735.

Hackett, J. A., Azim Surani, M. 2013. "DNA methylation dynamics during the mammalian life cycle". Philosophical Transactions of the Royal Society B: Biological Sciences.

Hardman, N. 1986. "Structure and function of repetitive DNA in eukaryotes.". The Biochemical Journal.

Hatziapostolou, M., Polytarchou, C., Aggelidou, E., Drakaki, A., Poultsides, G. A., Jaeger, S. A., … Iliopoulos, D. 2011. "An HNF4α-miRNA Inflammatory Feedback Circuit Regulates Hepatocellular Oncogenesis". Cell, *147*(6), 1233–1247.

Hodge, D. Q., Cui, J., Gamble, M. J., Guo, W. 2018. "Histone Variant MacroH2A1 Plays an Isoform-Specific Role in Suppressing EpithelialMesenchymal Transition". Scientific Reports, *8*(1).

Hollenhorst, P. C., McIntosh, L. P., Graves, B. J. 2011. "Genomic and Biochemical Insights into the Specificity of ETS Transcription Factors". Annual Review of Biochemistry, *80*(1), 437–471.

Iacono, G., Benevento, M., Dubos, A., Herault, Y., van Bokhoven, H., Nadif Kasri, N., Stunnenberg, H. G. 2017. "Integrated transcriptional analysis unveils the dynamics of cellular differentiation in the developing mouse hippocampus". Scientific Reports, *7*(1), 18073.

Jang, H. S., Shin, W. J., Lee, J. E., Do, J. T. 2017. "CpG and non-CpG methylation in epigenetic gene regulation and brain function". Genes.

Jeziorska, D. M., Murray, R. J. S., De Gobbi, M., Gaentzsch, R., Garrick, D., Ayyub, H., … Tufarelli, C. 2017. "DNA methylation of intragenic CpG islands depends on their transcriptional activity during differentiation and disease". Proceedings of the National Academy of Sciences of the United States of America.

Jia, D., Jolly, M. K., Kulkarni, P., Levine, H. 2017. "Phenotypic Plasticity and Cell Fate Decisions in Cancer: Insights from Dynamical Systems Theory". Cancers, *9*(12), 70.

Jia, D., Li, X., Bocci, F., Tripathi, S., Deng, Y., Jolly, M. K., … Levine, H. 2019. "Quantifying Cancer Epithelial-Mesenchymal Plasticity and its Association with Stemness and Immune Response". Journal of Clinical Medicine, *8*(5), 725.

Jin, B., Li, Y., Robertson, K. D. 2011. "DNA methylation: Superior or subordinate in the epigenetic hierarchy?". Genes and Cancer.

Jin, B., Robertson, K. D. 2013. "DNA methyltransferases, DNA damage repair, and cancer". Advances in Experimental Medicine and Biology.

Jing, Y., Han, Z., Zhang, S., Liu, Y., Wei, L. 2011. "Epithelial-Mesenchymal Transition in tumor microenvironment". Cell & Bioscience, *1*(1), 29.

Keller, G. 2005. "Embryonic stem cell differentiation: emergence of a new era in biology and medicine". Genes & Development, *19*(10), 1129–1155.

Kim, J. H., Shim, J. W., Eum, D. Y., Kim, S. D., Choi, S. H., Yang, K., … Park, M. T. 2017. "Downregulation of UHRF1 increases tumor malignancy by activating the CXCR4/AKT-JNK/IL-6/Snail signaling axis in hepatocellular carcinoma cells". Scientific Reports.

Klein, R. H., Lin, Z., Hopkin, A. S., Gordon, W., Tsoi, L. C., Liang, Y., … Andersen, B. 2017. "GRHL3 binding and enhancers rearrange as epidermal keratinocytes transition between functional states". PLOS Genetics, *13*(4), e1006745.

Kofunato, Y., Kumamoto, K., Saitou, K., Hayase, S., Okayama, H., Miyamoto, K., … Takenoshita, S. 2012. "UHRF1 expression is upregulated and associated with cellular proliferation in colorectal cancer". In *Oncology Reports*.

Kopp, J. L., Wilder, P. J., Desler, M., Kim, J.-H., Hou, J., Nowling, T., Rizzino, A. 2004. "Unique and Selective Effects of Five Ets Family Members, Elf3, Ets1, Ets2, PEA3, and PU.1, on the Promoter of the Type II Transforming Growth Factor-β Receptor Gene". Journal of Biological Chemistry, *279*(19), 19407–19420.

Kotarba, G., Taracha-Wisniewska, A., Wilanowski, T. 2020. "Grainyhead-like transcription factors in cancer – Focus on recent developments". Experimental Biology and Medicine, *245*(5), 402–410.

Kroepil, F., Fluegen, G., Totikov, Z., Baldus, S. E., Vay, C., Schauer, M., … Stoecklein, N. H. 2012. "Down-Regulation of CDH1 Is Associated with Expression of SNAI1 in Colorectal Adenomas". PLoS ONE, *7*(9), e46665.

Lafontaine, L., Chaudhry, P., Lafleur, M. J., Van Themsche, C., Soares, M. J., Asselin, E. 2011. "Transforming growth factor beta regulates proliferation and invasion of rat placental cell lines". Biology of Reproduction, *84*(3), 553–559.

Lamouille, S., Subramanyam, D., Blelloch, R., Derynck, R. 2013. "Regulation of epithelial–mesenchymal and mesenchymal–epithelial transitions by microRNAs". Current Opinion in Cell Biology, *25*(2), 200–207.

Lamouille, S., Xu, J., Derynck, R. 2014. "Molecular mechanisms of epithelialmesenchymal transition.". Nature Reviews. Molecular Cell Biology, *15*(3), 178–196.

Lavin, D. P., Tiwari, V. K. 2020. "Unresolved Complexity in the Gene Regulatory Network Underlying EMT". Frontiers in Oncology, *10*.

Liao, J., Karnik, R., Gu, H., Ziller, M. J., Clement, K., Tsankov, A. M., … Meissner, A. 2015. "Targeted disruption of DNMT1, DNMT3A and DNMT3B in human embryonic stem cells". Nature Genetics.

Lin, Y., Xu, J., Lan, H. 2019. "Tumor-associated macrophages in tumor metastasis: biological roles and clinical therapeutic applications". Journal of Hematology & Oncology, *12*(1), 76.

Liu, X., Gao, Q., Li, P., Zhao, Q., Zhang, J., Li, J., … Wong, J. 2013. "UHRF1 targets DNMT1 for DNA methylation through cooperative binding of hemimethylated DNA and methylated H3K9". Nature Communications.

Lombaerts, M., van Wezel, T., Philippo, K., Dierssen, J. W. F., Zimmerman, R. M. E., Oosting, J., … Cleton-Jansen, A.-M. 2006. "E-cadherin transcriptional downregulation by promoter methylation but not mutation is related to epithelial-to-mesenchymal transition in breast cancer cell lines". British Journal of Cancer, *94*(5), 661–671.

Lucarelli, M., Fuso, A., Strom, R., Scarpa, S. 2001. "The Dynamics of Myogenin Site-specific Demethylation is Strongly Correlated with its Expression and with Muscle Differentiation". Journal of Biological Chemistry.

Macara, I. G., Guyer, R., Richardson, G., Huo, Y., Ahmed, S. M. 2014. "Epithelial Homeostasis". Current Biology, *24*(17), R815–R825.

Maroulakou, I. G., Bowe, D. B. 2000. "Expression and function of Ets transcription factors in mammalian development: a regulatory network". Oncogene, *19*(55), 6432–6442.

Massague, J. 2008. "TGFbeta in Cancer.". Cell, *134*(2), 215–230. Retrieved from http://eutils.ncbi.nlm.nih.gov/entrez/eutils/elink.fcgi?dbfrom=pubmed&id=18662538&retmode=ref&cmd=prlinks%5Cnpapers2://publication/doi/10.1016/j.cell.2008.07.001%5Cnfile:///Users/Calixto/Papers2/Articles/2008/Massague/Cell/Cell 2008 Massague.pdf

Massenet, J., Gardner, E., Chazaud, B., Dilworth, F. J. 2021. "Epigenetic regulation of satellite cell fate during skeletal muscle regeneration". Skeletal Muscle.

Miettinen, P. J., Ebner, R., Lopez, A. R., Derynck, R. 1994. "TGF-β induced transdifferentiation of mammary epithelial cells to mesenchymal cells: Involvement of type I receptors". Journal of Cell Biology.

Mlacki, M., Kikulska, A., Krzywinska, E., Pawlak, M., Wilanowski, T. 2015. "Recent discoveries concerning the involvement of transcription factors from the Grainyhead-like family in cancer". Experimental Biology and Medicine, *240*(11), 1396–1401.

Monteiro-Reis, S., Lobo, J., Henrique, R., Jerónimo, C. 2019. "Epigenetic mechanisms influencing epithelial to mesenchymal transition in bladder cancer". International Journal of Molecular Sciences.

Moore, B. D., Khurana, S. S., Huh, W. J., Mills, J. C. 2016. "Hepatocyte nuclear factor 4α is required for cell differentiation and homeostasis in the adult mouse gastric epithelium". American Journal of PhysiologyGastrointestinal and Liver Physiology, *311*(2), G267–G275.

Moore, L. D., Le, T., Fan, G. 2013. "DNA methylation and its basic function". Neuropsychopharmacology.

Münzel, M., Globisch, D., Carell, T. 2011. "5-hydroxymethylcytosine, the sixth base of the genome". Angewandte Chemie - International Edition.

Nelson, W. J. 2009. "Remodeling epithelial cell organization: transitions between front-rear and apical-basal polarity.". Cold Spring Harbor Perspectives in Biology.

Newman, S. A. 2020. "Cell differentiation: What have we learned in 50 years?". Journal of Theoretical Biology, *485*, 110031.

Oka, M., Meacham, A. M., Hamazaki, T., Rodić, N., Chang, L. J., Terada, N. 2005. "De novo DNA methyltransferases Dnmt3a and Dnmt3b primarily mediate the cytotoxic effect of 5-aza-2′-deoxycytidine". Oncogene.

Oliver, J. R., Kushwah, R., Hu, J. 2012. "Multiple roles of the epitheliumspecific ETS transcription factor, ESE-1, in development and disease". Laboratory Investigation, *92*(3), 320–330.

Otero, M., Plumb, D. A., Tsuchimochi, K., Dragomir, C. L., Hashimoto, K., Peng, H., … Goldring, M. B. 2012. "E74-like Factor 3 (ELF3) Impacts on Matrix Metalloproteinase 13 (MMP13) Transcriptional Control in Articular Chondrocytes under Proinflammatory Stress". Journal of Biological Chemistry, *287*(5), 3559–3572.

Papin, C., Ibrahim, A., Le Gras, S., Velt, A., Stoll, I., Jost, B., … Hamiche, A. 2017. "Combinatorial DNA methylation codes at repetitive elements". Genome Research.

Patil, V., Ward, R. L., Hesson, L. B. 2014. "The evidence for functional nonCpG methylation in mammalian cells". Epigenetics.

Pliatska, M., Kapasa, M., Kokkalis, A., Polyzos, A., Thanos, D. 2018. "The Histone Variant MacroH2A Blocks Cellular Reprogramming by Inhibiting Mesenchymal-to-Epithelial Transition". Molecular and Cellular Biology, *38*(10).

Polo, J. M., Hochedlinger, K. 2010. "When Fibroblasts MET iPSCs". Cell Stem Cell, *7*(1), 5–6.

Probst, A. V., Dunleavy, E., Almouzni, G. 2009. "Epigenetic inheritance during the cell cycle". Nature Reviews Molecular Cell Biology.

Rajabi, H., Tagde, A., Alam, M., Bouillez, A., Pitroda, S., Suzuki, Y., Kufe, D. 2016. "DNA methylation by DNMT1 and DNMT3b methyltransferases is driven by the MUC1-C oncoprotein in human carcinoma cells". Oncogene.

Ramesh, S., Wildey, G. M., Howe, P. H. 2009. "Transforming growth factor β (TGFβ)-induced apoptosis: The rise & fall of Bim". Cell Cycle, *8*(1), 11– 17.

Redmer, T., Diecke, S., Grigoryan, T., Quiroga-Negreira, A., Birchmeier, W., Besser, D. 2011. "E-cadherin is crucial for embryonic stem cell pluripotency and can replace OCT4 during somatic cell reprogramming". EMBO Reports, *12*(7), 720–726.

Richa, R., Sinha, R. P. 2014. "Hydroxymethylation of DNA: An epigenetic marker". EXCLI Journal.

Robert, M. F., Morin, S., Beaulieu, N., Gauthier, F., Chute, I. C., Barsalou, A., MacLeod, A. R. 2003. "DNMT1 is required to maintain CpG methylation and aberrant gene silencing in human cancer cells". Nature Genetics.

Roca, H., Hernandez, J., Weidner, S., McEachin, R. C., Fuller, D., Sud, S., … Pienta, K. J. 2013. "Transcription Factors OVOL1 and OVOL2 Induce the Mesenchymal to Epithelial Transition in Human Cancer". PLoS ONE, *8*(10), e76773.

Salviano-Silva, A., Lobo-Alves, S. C., de Almeida, R. C., Malheiros, D., PetzlErler, M. L. 2018. "Besides pathology: Long non-coding RNA in cell and tissue homeostasis". Non-Coding RNA.

SanMiguel, J. M., Bartolomei, M. S. 2018. "DNA methylation dynamics of genomic imprinting in mouse development†". Biology of Reproduction.

Santiago, M., Antunes, C., Guedes, M., Sousa, N., Marques, C. J. 2014. "TET enzymes and DNA hydroxymethylation in neural development and function - How critical are they?". Genomics.

Saydam, O., Shen, Y., Würdinger, T., Senol, O., Boke, E., James, M. F., … Breakefield, X. O. 2009. "Downregulated MicroRNA-200a in Meningiomas Promotes Tumor Growth by Reducing E-Cadherin and Activating the Wnt/β-Catenin Signaling Pathway". Molecular and Cellular Biology, *29*(21), 5923–5940.

Schermelleh, L., Haemmer, A., Spada, F., Rösing, N., Meilinger, D., Rothbauer, U., … Leonhardt, H. 2007. "Dynamics of Dnmt1 interaction with the replication machinery and its role in postreplicative maintenance of DNA methylation". Nucleic Acids Research.

Sengez, B., Aygün, I., Shehwana, H., Toyran, N., Tercan Avci, S., Konu, O., … Alotaibi, H. 2019. "The Transcription Factor Elf3 Is Essential for a Successful Mesenchymal to Epithelial Transition". Cells, *8*(8), 858.

Shu, X., Pei, D. 2014. "The function and regulation of mesenchymaltoepithelial transition in somatic cell reprogramming". Current Opinion in Genetics & Development, *28*, 32–37.

Sisto, M., Lisi, S., Ribatti, D. 2018. "The role of the epithelial-to-mesenchymal transition (EMT) in diseases of the salivary glands". Histochemistry and Cell Biology, *150*(2), 133–147.

Skrypek, N., Goossens, S., De Smedt, E., Vandamme, N., Berx, G. 2017. "Epithelial-to-Mesenchymal Transition: Epigenetic Reprogramming Driving Cellular Plasticity". Trends in Genetics, *33*(12), 943–959.

Stemmler, M. P., Hecht, A., Kemler, R. 2005. "E-cadherin intron 2 contains cisregulatory elements essential for gene expression". Development.

Stemmler, M. P., Hecht, A., Kinzel, B., Kemler, R. 2003. "Analysis of regulatory elements of E-cadherin with reporter gene constructs in transgenic mouse embryos". Developmental Dynamics.

Subramaniam, D., Thombre, R., Dhar, A., Anant, S. 2014. "DNA methyltransferases: A novel target for prevention and therapy". Frontiers in Oncology.

Tajima, S., Suetake, I., Takeshita, K., Nakagawa, A., Kimura, H. 2016. "Domain structure of the Dnmt1, Dnmt3a, and Dnmt3b DNA methyltransferases". Advances in Experimental Medicine and Biology.

Takaishi, M., Tarutani, M., Takeda, J., Sano, S. 2016. "Mesenchymal to Epithelial Transition Induced by Reprogramming Factors Attenuates the Malignancy of Cancer Cells". PLOS ONE, *11*(6), e0156904.

Teeuwssen, M., Fodde, R. 2019. "Cell Heterogeneity and Phenotypic Plasticity in Metastasis Formation: The Case of Colon Cancer". Cancers, *11*(9), 1368.

Thiery, J. P., Acloque, H., Huang, R. Y. J., Nieto, M. A. 2009. "Epithelialmesenchymal transitions in development and disease.". Cell, *139*(5), 871–890.

Thomas, P., Popović, N., Grima, R. 2014. "Phenotypic switching in gene regulatory networks". Proceedings of the National Academy of Sciences, *111*(19), 6994–6999.

Tian, F.-Y., Marsit, C. J. 2018. "Environmentally Induced Epigenetic Plasticity in Development: Epigenetic Toxicity and Epigenetic Adaptation". Current Epidemiology Reports, *5*(4), 450–460.

Tymms, M. J., Ng, A. Y. N., Thomas, R. S., Schutte, B. C., Zhou, J., Eyre, H. J., … Kola, I. 1997. "A novel epithelial-expressed ETS gene, ELF3: human and murine cDNA sequences, murine genomic organization, human mapping to 1q32.2 and expression in tissues and cancer". Oncogene, *15*(20), 2449–2462.

van Roy, F., Berx, G. 2008. "The cell-cell adhesion molecule E-cadherin". Cellular and Molecular Life Sciences, *65*(23), 3756–3788.

Varga, J., Greten, F. R. 2017. "Cell plasticity in epithelial homeostasis and tumorigenesis". Nature Cell Biology.

Varriale, A. 2014. "DNA Methylation, Epigenetics, and Evolution in Vertebrates: Facts and Challenges". International Journal of Evolutionary Biology.

Wasylyk, B., HAHN, S. L., GIOVANE, A. 1993. "The Ets family of transcription factors". European Journal of Biochemistry, *211*(1–2), 7–18.

Wendt, M. K., Allington, T. M., Schiemann, W. P. 2009. "Mechanisms of the epithelial–mesenchymal transition by TGF-β". Future Oncology, *5*(8), 1145–1168.

Weyemi, U., Redon, C. E., Choudhuri, R., Aziz, T., Maeda, D., Boufraqech, M., … Bonner, W. M. 2016. "The histone variant H2A.X is a regulator of the epithelial-mesenchymal transition". Nature Communications, *7*.

Wu, H., Zhang, Y. 2014. "Reversing DNA methylation: Mechanisms, genomics, and biological functions". Cell.

Xu, J., Lamouille, S., Derynck, R. 2009. "TGF-B-induced epithelial to mesenchymal transition". Cell Research.

Yamada, Y., Watanabe, H., Miura, F., Soejima, H., Uchiyama, M., Iwasaka, T., … Ito, T. 2004. "A comprehensive analysis of allelic methylation status of CpG islands on human chromosome 21q". Genome Research.

Yao, D., Dai, C., Peng, S. 2011. "Mechanism of the Mesenchymal–Epithelial Transition and Its Relationship with Metastatic Tumor Formation". Molecular Cancer Research, *9*(12), 1608–1620.

Yao, D., Peng, S., Dai, C. 2013. "The role of hepatocyte nuclear factor 4alpha in metastatic tumor formation of hepatocellular carcinoma and its close relationship with the mesenchymal–epithelial transition markers". BMC Cancer, *13*(1), 432.

Zhang, H., DiBaise, J. K., Zuccolo, A., Kudrna, D., Braidotti, M., Yu, Y., … Krajmalnik-Brown, R. 2009. "Human gut microbiota in obesity and after gastric bypass". Proceedings of the National Academy of Sciences, *106*(7), 2365–2370.

Zhang, J., Tian, X. J., Xing, J. 2016. "Signal transduction pathways of EMT induced by TGF-β, SHH, and WNT and their crosstalks". Journal of Clinical Medicine.

Zhang, Y., Alexander, P. B., Wang, X. F. 2017. "TGF-β family signaling in the control of cell proliferation and survival". Cold Spring Harbor Perspectives in Biology, *9*(4).

8. APPENDIX

Table 13. Cloning Primer Sequences with restriction sites.

	Primer Sequence	Restriction Sites
Dnmt1_F	acgtGAGCTCatattggtccagttcacttc	SacI
Dnmt1_R	cactCTCGAGtagtgggctcgtccgtgctg	XhoI
Dnmnt1_p-addsite_F	ttggtgcatttaagagcagtgtc	No site
Dnmt1_p-add-site_R	tccaAAGCTTcggccgcagggccacccggag	HindIII
Dnmt3b_F	acgtGCTAGCgccacctctgccccgctag	NheI
Dnmt3b_R	cactCTCGAGgggcggcgccgctgcccttgta	XhoI
Uhrf1_F	acgtGAGCTCctagttattgcacagatgcc	NheI
Uhrf1_R	cactCTCGAGtgattcctgattggctggcg	XhoI

Table 14. qPCR Primers and Probe informations.

	Primer Sequence	Probe
Dnmt1_F	TGGCAAGCAAACCAGAGTCA	132
Dnmt1_R	TTGCCTGAAGAGGTGGCTC	132
Dnmt3b_F	GTCGAAAAGCCAATGCAGGG	120
Dnmt3b_R	TTCACAGGTCTGGATGAGCG	120
Uhrf1_F	TCAGAAGTCTCGGGGTGGT	14
Uhrf1_R	CTGCCGGCTATGCTCACTT	14
Elf3_F	ACCGAACCCTGACACACCT	46
Elf3_R	AGCTGTACATGGCGTTGAAGT	46
Cdh1_TSS_F	TGAGTTCCCAAGAACTTCTGC	51
Cdh1_TSS_R	GCCGAGCAAACACTGAGC	51
Cdh1_14100_F	CCCTTGGTTCTAAAGTTGGTTG	107
Cdh1_14100_R	GGAATGAGGAAACTGGTTTGAC	107
Grhl3_Prom_F	TCTAGTTCTCCCGTTCCTTCC	52
Grhl3_Prom_R	TTCTTAGCTGAGGGGGTGAG	52
Grhl3_Prom_2_F	GGAGAAAAGAGAGGGGACTCA	108
Grhl3_Prom_2_R	TCACCTTCTCTACCCGGAAA	108
Ovol2-P_F	GCAAACATTCATGCCTAAGGA	27
Ovol2-P_R	AACAAGCTCGCTACCTGTCC	27
Cebpa260_F	CTCCCCAACCTCCACCTC	11
Cebpa260_R	CCTCCTTTAAGCCTCTAAGTCACC	11
Hnf4a-P2_R	ATGTCAGCTGGGTTGTCCAC	66
Hnf4a-P2_F	AACAGGACTGGCATTGGTTG	66
Snai1-P_F	GTTCCAGGAACCCCTAAGCG	129

Snai1-P_R	CCCGAGCTGCTGACCTTT	129
Zeb2-P_F	CTGGATAAAGGGCAGGGAGG	52
Zeb2-P_R	TCGCCTGGGGATTGGAAAC	52
Cdh1_F	ATCCTCGCCCTGCTGATT	18
Cdh1_R	ACCACCGTTCTCCTCCGTA	18

Snai1_ F	CTTGCTCCACAAGCACCA	71
Snai1_ R	GAGGATGGGGAGGTAGCAG	71
Zeb1_ F	TGGAGTTCAAAGGTTGTCGTT	109
Zeb1_ R	TTGCCACATCAACACTGGTC	109
Zeb2_ F	TTGCTCCAGGATGTGTGG	64
Zeb2_ R	CACACACTTGTTTGTGTGCATATC	64
Hnf4a_ F	AGCCTAAATGACAGGTCCTCTG	73
Hnf4a_ R	TTAATCAGCTGGCCCCATT	73
Ovol2_F	GTGAGGATTGCGGCTACAC	79
Ovol2_R	TGGTCACTGTTCACATGCAG	79

İZMİR BİYOTIP VE GENOM MERKEZİ
GİRİŞİMSEL OLMAYAN ARAŞTIRMALAR ETİK KURULU (İBG-GOEK)
KARARI

Toplantı Tarihi	: 26/05/2023	**Toplantı Günü**	: Cuma
Toplantı Sayısı	: 6	**Toplantı Saati**	: 10:30

Sayın Dr. Hani ALOTAIBI,

2023-013 Protokol No'lu; sorumlusu olduğunuz "Mezenkimal Epitelyal Dönüşüm Sürecinde Elf3 ve DNA Metil Transferazların Etkileşimleri" başlıklı araştırmanın uygulanmasında etik açıdan sakınca olmadığına oy birliği ile karar verilmiştir.

Bilgilerinizi ve gereğini rica ederiz.

Prof. Dr. H. Alper BAĞRIYANIK **Başkan**	**Prof. Dr. Hilmi ORHAN** **Başkan Yardımcısı**
Prof. Dr. Sedef AKGÜNGÖR **Üye** (Katılmadı)	**Prof. Dr. Gülgün OKTAY** **Üye**
Dr. Serap ERKEK ÖZHAN **Üye** (Katılmadı)	**Prof. Dr. Şermin GENÇ** **Üye**
Doç. Dr. Canan Aslı YILDIRIM **Üye**	**Doç. Dr. Can KÜÇÜK** **Üye** (Katılmadı)
Dr. Öğr. Üyesi Yavuz OKTAY **Üye**	

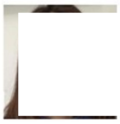

SERAY YETKİN

Personal Information

Contact Information

Contact Address	Doku ... enome Center, 58/5
Telephone	(531)
Email	yetki
Web Page	

Education Information

01 September 2021 - Now (2 Year 1 Month)
Yüksek Lisans, Tezli Program, DOKUZ EYLÜL ÜNİVERSİTESİ, TÜRKİYE
İZMİR ULUSLARARASI BİYOTIP VE GENOM ENSTİTÜSÜ, BİYOTIP VE SAĞLIK TEKNOLOJİLERİ (YL) (TEZLİ) (İNGİLİZCE)
Cumulative Grade Point Average: 4.0 / 4.0

01 August 2016 - 01 June 2021 (4 Year 11 Month)
Lisans, Anadal/Normal Öğretim, ÇANAKKALE ONSEKİZ MART ÜNİVERSİTESİ, TÜRKİYE
FEN VE EDEBİYAT FAKÜLTESİ, MOLEKÜLER BİYOLOJİ VE GENETİK BÖLÜMÜ
Cumulative Grade Point Average: 3.31 / 4.0

Foreign Language Information

İNGİLİZCE (Reading: İyi, Writing: Orta, Speaking: Orta)

ALMANCA (Reading: Başlangıç, Writing: Başlangıç, Speaking: Başlangıç)

R&D Competency

Articles

S. YETKİN & H. ALOTAİBİ, Selection and validation of novel stable reference genes for qPCR analysis in EMT and MET, EXPERIMENTAL CELL RESEARCH, 2023, 0014-4827, 428, 1.

B. SUCU, A. BAYRAKTAR, H. DUMAN, A. ARSLAN, M. KAPLAN, M. KARYELİOGLU, E. NTELİTZE, T. TASTEKİN, S. YETKİN, M. ERTURK, S. A. FRESE, B. M. HENRİCK, H. M. KAYİLİ, B. SALİH & S. KARAV, Recombinant Production of Bifidobacterial Endoglycosidases for N-glycan Release, JOVE-JOURNAL OF VISUALIZED EXPERIMENTS, 2021, 1940-087X, 173.

TÜBİTAK Scholarships and Fundings

Project Info	122Z886, Mezenkimal Epitelyal Dönüşüm Sürecinde Rol Alan Mikrorna'Ların Tanımlanması Ve Fonksiyonel Analizleri, Burslu, Yürürlükte, KBAG - Kimya Biyoloji Araştırma Destek Grubu, 1001 - Araştırma, ARDEB, Project Participation/Leave Dates: 4/6/23 - 9/8/23, Project Start/End Dates: 3/15/23 - 3/15/26. 120N556, Mezenkimal Epitelyal Dönüşümün Epigenetiği, Burslu, Yürürlükte, UPAG - Uluslararası Işbirliği Projeleri Araştırma Destek Grubu, Uluslararası / PIA-Bosphorus-Fransa, ARDEB, Project Participation/Leave Dates: 9/29/21 - 8/22/22, Project Start/End Dates: 3/1/21 - 3/1/23. 219Z034, Mezenkimal Epitelyal Dönüşüm Sürecinde Kritik Olan Uzun Kodlamayan RNA'ların İşlevsel Analizleri, Burslu, Yürürlükte, KBAG - Kimya Biyoloji Araştırma Destek Grubu, 1001 - Araştırma, ARDEB, Project Participation/Leave Dates: 8/22/22 - 4/6/23, Project Start/End Dates: 7/15/20 - 7/15/23. 118Z146, Farklı Tekniklerle Aktivitesi Manipüle Edilmiş Yeni Bacteroides ve Bifidobakteri Glikosidazları Yardımıyla Glikanların Glikoproteinlerin Biyolojik Özelliklerine Olan Katkılarının Belirlenmesi, Burslu, Yürürlükte, KBAG - Kimya Biyoloji Araştırma Destek Grubu, 1001 - Araştırma, ARDEB, Project Participation/Leave Dates: 10/15/20 - 7/1/21, Project Start/End Dates: 1/15/19 - 4/15/23.
BIDEB Supports	SERAY YETKİN, Araştırma Burs ve Destekleri Müdürlüğü, 2209-A Üniversite Öğrencileri Araştırma Projeleri Destekleme Programı, Destek Sona Erdi, 2020 - 1.

Number of Panelist/Observer/Reporter Jobs

Refereeing/Panelist/Outer Consultant Count	ARDEB/BİDEB 0	TEYDEB 0	Total 0
Number of Observer/Consultant Jobs	ARDEB/BİDEB 0	TEYDEB 0	Total 0
Number of Reporter Jobs	ARDEB/BİDEB 0	TEYDEB 0	Total 0